

# Port Valdez Weather Buoy Data Analysis

Report submitted by:

Robert W. Campbell, Ph.D.

PO Box 1693

Cordova, AK

99574

[rcampbell@pwssc.org](mailto:rcampbell@pwssc.org)

(907) 253-7621

August 2, 2021



## Contents

List of Acronyms .....	2
Executive Summary .....	2
Introduction.....	2
Data operations, notes, and QA/QC.....	3
A primer on the visualization of vector data.....	4
Results and discussion .....	5
Air and Sea Surface Temperature .....	5
Relative humidity .....	5
Barometric pressure.....	5
Solar radiation .....	6
Wind speed and direction, wind gusts.....	6
Wave height and direction.....	7
Temperature climatology .....	7
Surface Currents.....	8
Conclusions.....	10
Literature cited .....	12
Figures.....	13
Appendix 1: Table of averages and minimum/maximum values at the VMT buoy, by month. ..	37
Appendix 2: Table of averages and minimum/maximum values at the Duck Flats buoy, by month. ....	38

### List of acronyms used in this report

GS16	De-tiding method developed by Gargett and Savidge (2016)
NOAA	National Oceanic and Atmospheric Administration
CO-OPS	Center for Operational Oceanographic Products and Services, NOAA
PWS	Prince William Sound
PWSRCAC	Prince William Sound Regional Citizens' Advisory Council
QA/QC	Quality Assurance / Quality Control
VDZA2	NOAA tide station in Valdez Harbor
VMT	Valdez Marine Terminal
WMO	World Meteorological Organization

### Executive summary

Two buoys were deployed in Port Valdez in 2019 by PWSRCAC, one adjacent to the Valdez Marine Terminal (VMT), and one near the Valdez Duck Flats. Time series of the meteorological and oceanographic observations at each of the buoys were analyzed for seasonal, intra-, and interannual patterns. Solar radiation, air, and water temperatures all showed a cyclical seasonal progression typical to subarctic regions, with minima in February and maxima in August. Relative humidity was high, as befits a coastal region with a large amount of annual precipitation, and tended to follow temperature trends. Air pressure, driven by large scale atmospheric circulations, was similar between the two sites. Winds were primarily from the east in autumn and winter, again driven by the large scale atmospheric patterns that create a low pressure system over the Gulf of Alaska during that time. In late spring and summer, daily westerly sea breezes were common. A 112-year-long temperature climatology was constructed for the Valdez region, which showed a steady and persistent warming trend. Temperatures in 2019 tended towards warmer than average and transitioned towards cooler than average in 2020, as did much of the North Pacific, in response to a La Niña event. Although surface currents have a tidal component, several attempts to remove high frequency tidal variability and examine low frequency circulations were not particularly successful, in part due to gaps in the time series and perhaps also due to other high frequency components such as winds. Residual circulations that were extracted were very small. Compared to the VMT, currents at the Duck Flats location were quite weak. Cross covariance analysis comparing the timing of currents at the buoys compared to the tides at the Port Valdez tide station showed that surface currents tended to lag the tides by approximately 45 minutes.

### Introduction

The Prince William Sound Regional Citizens' Advisory Council (PWSRCAC) operates two weather buoys in Port Valdez, one offshore of the Valdez Marine Terminal (VMT) at Jackson Point that was deployed in May 2019, and one adjacent to the Valdez Duck Flats that was deployed in September 2019 (figure 1). Both buoys have been uploading meteorological and oceanographic observations on an hourly basis (with some interruptions due to hardware/software failures and service visits) since their deployment.

Standard equipment on each buoy includes an anemometer, relative humidity sensor, three temperature thermistors (one dedicated for air temperature, a secondary included in the relative humidity sensor, and one to measure sea surface temperature mounted ~1 meter (m) below the

waterline), barometer, radiometer, Acoustic Doppler Current Meter (for surface currents), and a wave sensor (only on the VMT buoy at present). An onboard electric compass is used to measure the buoy heading to adjust direction measurements (wind, waves, and current) to true north. The measured parameters of interest, their units, and recording period are listed in Table 1.

Table 1: Meteorological and oceanographic parameters collected by the buoys.

Parameter	Instrument Make/Model	Units	Recording period
Wind speed	RM Young 05103-L	m/s	6 minutes
Wind gust speed	RM Young 05103-L	m/s	6 minutes
Wind direction	RM Young 05103-L	Deg. True	6 minutes
Air temperature	Campbell Scientific 109	°C	15 minutes
Relative humidity	Campbell Scientific HC2S	%	15 minutes
Barometric pressure	Setra CS100-QD	mbar	15 minutes
Solar radiation	Hukseflux LP02	W/m <sup>2</sup>	15 minutes
Current speed	Nortek Aquadopp 2 MHz	m/s	20 minutes
Current direction	Nortek Aquadopp 2 MHz	Deg. True	20 minutes
Significant wave height	Axys TriAXYS	m	Hourly
Maximum wave height	Axys TriAXYS	m	Hourly
Wave period	Axys TriAXYS	s	Hourly
Wave direction	Axys TriAXYS	Deg. True	Hourly

The high frequency of sampling by the buoys has already created large archive of observations, approximately 3.7 million primary data points for the VMT buoy and 3.3 million data points for the Duck Flats buoy, plus a similar amount of associated metadata. The purpose of this report is to provide a preliminary analysis of some of the seasonal and higher frequency patterns found in the data.

This report is structured around the different data types produced by the buoys. Following discussion with PWSRCAC staff and committee members, the basic averaging period was decided to be monthly. In some cases higher frequencies have been used where appropriate to provide a higher level of detail. Given the very broad backgrounds of the many PWSRCAC stakeholders, it has been attempted to avoid or explain technical jargon where possible to provide a plain language interpretation for that large and diverse audience. Rather than the usual methods/results/discussion format featured in the scientific literature, a more narrative structure was adopted and explanations of methods, highlighting of the results and discussion of them, have been done all at the same time for the many different data collected. The metric units used by the buoys have also been mostly converted to imperial units. Graphical presentations of the data have been used as much as possible and a tabular compilation of monthly averages at both buoys has also been included in appendices.

### Data operations, notes, and QA/QC

All data was downloaded directly from the buoy servers. Each time series was examined with automated and manual methods for anomalous spikes. Relative humidity values prior to January 2020 at the VMT were removed (the sensor was damaged) and occasional bad water temperature

observations at the buoys (less than 28°F) were removed. On or about March 11, 2020, the VMT buoy had a power issue which tripped the main fuse from the battery, which resulted in intermittent daytime-only data (when the solar panels produced enough voltage to power up the data logger) until the buoy was repaired on April 29.

### **A primer on the visualization of vector data**

Meteorological and oceanographic data are either scalar observations (magnitude only, e.g., temperature) or vector observations (magnitude and direction, e.g., winds). Scalar data may be visualized with a standard x-y plot that should be familiar to most. Vector data, having two components, is more complicated to visualize. A vector may be visualized as an arrow, with the direction indicated by the direction the arrow is pointed, and the magnitude indicated by the length of the arrow (figure 2A). When doing mathematical operations on a vector, vectors are usually broken up into components that correspond to the dimensions of the vector. The red and blue arrows in figure 2A indicate those two components for the two dimensional vector shown: there is a horizontal component and a vertical component. Those components are usually designated as ‘u’ and ‘v’ in the technical literature and in the context of meteorological data are referred to as the zonal (i.e., “east-west”) and meridional (i.e., “north-south”) components. In this context positive numbers mean one direction and negative numbers mean the opposite. For example, on the east-west axis a positive number is eastward and a negative number is westward.

Averaging of vector observations is usually done on the components and then may be visualized in a number of ways. The two methods used in this report are roses and quiver plots. A rose is a good way to summarize a large number of observations and may be thought of as something similar to a bar chart, but arranged in a circle to indicate directions. An example of a rose plot is shown in figure 2B, which represents all the wind observations made by the VMT buoy in the month of June 2020. The wind directions (the direction the wind is blowing from) are broken up into 10-degree “bins” that are shown by the bars. The length of the bars is proportional to the frequency of winds blowing from that direction and the colors indicate bins of wind speeds, which are shown in the color scale to the right. Figure 2B shows us that most of the winds in June 2020 were primarily in the east-west direction. The median wind direction (i.e., the most frequent, shown by the longest bar) was just south of westerly. The four largest bars showing westerly to southwesterly winds can be summed up on the circular scale and show that something like half (50%) of winds were in those westerly to southwesterly directions. The color scale shows that the strongest winds were westerlies with a small proportion blowing 15-20 knots (green bars), slightly more blowing 10-15 knots (cyan bars), and more still blowing 5-10 knots (light blue bars). One can also see that easterly winds were generally weak, being mostly 0-5 knots (dark blue bars).

Quiver plots allow examining finer scale patterns that would be impractical with rose plots; quiver plots show a vector as an arrow or a line. An example quiver plot is shown in figure 2C, again using wind data from June 2020 at the VMT buoy, but with daily average wind speed and direction shown. Each arrow in the plot is the daily average wind velocity with the angle of the stick showing the direction of the wind vector and the length of the stick indicating the wind speed. The axis is scaled such that the length of the stick is proportional to the ticks on the bottom axis. Because the winds, waves, and currents in Port Valdez are primarily oriented in the east-west direction, the

plots were produced with time shown vertically. Arrowheads are shown in the example plot, but are not shown in the rest of plots in this report because they show a great deal more data and the arrowheads tended to add clutter that made the plots more difficult to read.

Meteorologists and oceanographers use different conventions when speaking of directions: meteorologists speak of the direction that winds are coming from (e.g., a northerly wind is coming from the north), while oceanographers speak of the direction water is traveling too (e.g., an eastward current is travelling to the east). This convention has been adhered to in this report for the rose plots, but has not for the quiver plots, because the quiver plots are a direct representation of the vector in question (the average movement of the air or water). This is why the rose in figure 2B has bars pointing to the left (“winds from”), while the quiver plot in figure 2C has vectors pointing to the right (“direction air is moving to”). In the text of this report both “from” and “to” notation is used depending on the convention (meteorological vs oceanographic).

## **Results and discussion**

### *Air and Sea Surface Temperature*

Monthly air and water temperatures at both buoys showed the typical sinusoidal seasonal cycle expected in a subarctic environment (figures 3 and 4), with maxima in August and minima in February and considerable day-to-day departures from monthly means. Air temperatures tended to be slightly higher at the VMT buoy (figure 3) than at the Duck Flats buoy (figure 4), which may indicate a slightly more terrestrial influence at the Duck Flats buoy (e.g., downsloping winds from the Valdez Glacier Valley, see winds discussion below). Water temperatures were also slightly cooler at the Duck Flats, which likely reflects potential source waters from the Lowe and Valdez Glacier Rivers, which can be expected to be cooler than seawater given the presence of year-round ice in their watersheds.

### *Relative humidity*

Relative humidity was variable at both sites (figures 3 and 4). Much of the time relative humidity was quite high, greater than 70%, as befits the coastal climate both buoys are measuring. Part of the data record from the VMT was removed for data quality issues, but both buoys have an almost complete record from 2020, and the patterns between the buoys are quite similar, suggesting that although noisy, the observations are likely valid. Relative humidity was highest in August and lowest in March, following the temperature cycle.

### *Barometric pressure*

Air pressure was very similar between both sites, as would be expected because air pressure is largely driven by large scale atmospheric circulations (figures 3 and 4). There was not a strong seasonal cycle in air pressure. Air pressure in summer 2019 was quite high, and likely driven by a large scale atmospheric ridge that set up over the north Gulf Coast that year (Amaya et al., 2020). A similar pattern set up in 2020. Pressure was more variable in the autumn months, with the onset of so-called “equinox weather” which tends to feature large cyclonic circulations driven by the Aleutian Low, which usually sets up in the Gulf of Alaska in autumn and winter and determines the storm tracks to the region (Rodionov et al., 2007).



### *Solar radiation*

As to be expected given the latitude of the sites, solar radiation was strongly seasonal, peaking in June and with a nadir during the winter months (figures 3 and 4). Both buoys are shaded by the mountains fringing Port Valdez during the late autumn and winter months, which has created some power issues (both buoys are powered by solar panels), particularly at the VMT. The intermittent values in March and April 2020 (collected only during days when the solar panel energized the logger) resulted in spuriously large averages for those months because only daytime values were collected.

### *Wind speed and direction, wind gusts*

Winds are summarized as monthly wind roses (figures 5 and 6), and following meteorological convention are shown as the direction the wind is blowing from (i.e., an east wind blows from the east). The anemometers on the buoys are very sensitive and usually move slightly in all but the calmest conditions. They are also subject to freezing up after heavy snow and rain events followed by freezing temperatures. This manifests as a zero wind speed from exactly true north (vector multiplication on the 0 wind speed results in a direction of 0 as well) and can be seen on the wind roses as a spike in observations at the 0-degree band only. Those spikes may be used as an indicator of the frequency of calms during summer months and freeze-up events in winter.

Both the roses and the quiver plots (figures 7 and 8) show that most winds were easterly during autumn and winter and transitioned to westerlies from May until August at both buoys. The strongest winds were easterlies, during the autumn and winter months, likely driven by outflow winds caused by the large scale atmospheric features that set up in autumn/winter (the Aleutian Low offshore and high pressure over the interior). The summer westerlies are a daily sea breeze caused by localized heating and cooling that is familiar to mariners in the region (Lethcoe and Lethcoe, 2009). During the day, the sun heats the land faster than the ocean, creating upward convection and low air pressure over land; this draws air in from the ocean and creates a landward breeze (from the west in Port Valdez). At night, the land cools faster than the ocean, creating convection in the opposite direction. To illustrate this, hourly average winds in the east-west direction in May and June 2020 are shown in figure 9. Westerly winds are depicted with a green color scale and easterly winds are depicted with a blue color scale. On most days, winds were easterly from midnight until approximately 10 a.m., then switched to westerlies into the afternoon and evening.

The roses and quiver plots also show that wind directions were not completely symmetrical. There was a northerly component as well, regardless of if the winds were primarily from the east or west. That slight northerly tendency may have been caused by topographic steering of the winds by the steep terrain of Port Valdez, with westerly winds blowing out of Shoup Bay to the northwest. The northeastern cant of easterly winds may indicate that winds from Valdez Glacier valley tend to predominate over those of the Lowe river valley at the Duck Flats location.

Following the World Meteorological Organization (WMO) standard, the buoys also recorded a running 3 second average wind speed and reported the maximum of that 3 second average in each 6 minute wind recording period as the wind gust speed. Upon examination, a number of unrealistic (greater than 200 knots) gust observations were found in the gust time series, those values have been traced to an incorrect setting in wind measurement lines in the original data logger program

provided by the builder of the buoys (the setting was corrected in February 2021). The relationship between wind speed and wind gusts at National Data Buoy Center weather buoys in Prince William Sound (PWS) and at shore stations in Port Valdez were examined and it was found that wind gusts exceeding 3 times the wind speed were exceedingly rare. Gusts exceeding 3 times the wind speed in the buoy time series were accordingly discarded. The wind gust time series at the buoys (figure 10) followed the same pattern as sustained winds, with maximums during the winter months and elevated gusts during the summer westerly season. Summer gust speeds were in the 15-20-knot range and 40-50-knot gusts occurred during autumn and winter storms.

### *Wave height and direction*

Wave observations have also been summarized as roses (figures 11 and 12) and quiver plots (figures 13 and 14). Wind makes waves and the wave observations reflect the wind observations, with most waves, and the largest waves, from the east at the VMT during the winter months and from the west in spring and summer. The time series at the Duck Flats is quite short as the wave sensor was destroyed by the April 2020 power spike and has not been replaced. Waves at the Duck Flats were also primarily from the west and from the northeast in winter. Being deployed at the extreme eastern end of Port Valdez, the Duck Flats buoy has essentially no fetch to the east (it is approximately 1/10<sup>th</sup> of a mile from shore: figure 1). The waves from the southeasterly direction thus likely represent refraction of waves created in the southeast corner of Port Valdez during strong winter easterlies. Wave heights at the Duck Flats were also smaller than at the VMT as the Duck Flats site is partially protected from winds from the northwest.

The largest maximum wave height observed in the time series was an observation of just under 7 feet in March 2020 at the VMT. Maximum summertime wave heights at the VMT ranged between 1 and 3 feet and were slightly higher during winter storms. The short time series at the Duck Flats spanned the 2019/2020 winter and maximum wave heights in the 3-4-foot range were observed.

### **Temperature climatology**

Although the buoys have a fairly short time series, in order to put the buoy observations into a climatological context it is possible to convert observations into anomalies (i.e., departures from the long-term average) using observations from nearby stations, with the assumption that they are reasonably similar. There is a National Oceanic and Atmospheric Administration (NOAA) Center for Operational Oceanographic Products and Services (CO-OPS) weather and water level station in Valdez harbor, named VDZA2, which has a record of water temperatures that goes back to 2009. An average annual temperature cycle based on weekly averages was created from the VDZA2 time series (figure 16) to use as a long-term average.

Water temperatures at the buoys may then be averaged by each week and subtracted from the weekly averages at VDZA2 to produce an anomaly plot (figure 17), which depicts the departure of observations from the long-term average and with the seasonal cycle removed. The anomaly plot shows that relative to the 2009-2020 average, surface waters were much warmer than average in the early summers of both 2019 and 2020 at the VMT but tended to be cooler than average in autumn in both years. This matches with larger scale oceanographic patterns seen elsewhere, including a Gulf of Alaska wide marine heat wave in 2019 (Amaya *et al.* 2020) and warm surface waters observed in PWS in 2020 (Campbell, *unpubl. obs*); the trend towards cooler temperatures



in the latter portion of 2020 may be related to the ongoing La Niña event (NOAA CPC 2020). La Niña events are usually correlated with cooler surface temperatures in the North Pacific (Papineau, 2001; Newman et al., 2016), but PWS tends to lag the Gulf of Alaska by about a year in terms of temperature responses (Campbell, 2018). The difference between the anomalies at the two buoys may be attributed in part to the differences in water temperatures observed by the buoys with cooler temperatures found at the Duck Flats (see above, figures 3 and 4).

Although the water temperature record is comparatively short, a longer climatology is available for monthly average air temperatures in Valdez that was compiled by the Berkeley Earth database (<http://berkeleyearth.org/>). The Berkeley Earth time series spans from 1908 to 2013, using data from several National Weather Service and Federal Aviation Administration weather stations that have existed in the Valdez area over the years. To bring the climatology all the way to present day, the VDZA2 air temperature time series was appended to the Berkeley Earth one. The Berkeley Earth climatology overlaps with the VDZA2 time series for several years, which permits examining for offsets between the two time series. A linear regression comparing monthly averages at the VDZA2 station to the Berkeley Earth averages (figure 18) showed a very tight relationship between the two (with the exception of one outlier), but with a significant slope and offset. This suggests that although the two data sets showed the same pattern, there were slight differences in the temperatures that they estimated. The Berkeley Earth averages were therefore adjusted with the slope and intercept to make them consistent with the contemporary VDZA2 record.

The complete time series of air temperature anomalies from 1908 to 2020 (figure 19) shows a consistent warming trend of just under a half of a degree Fahrenheit per decade over the last 112 years, an overall increase in average temperatures of 5 degrees. This is consistent with trends observed elsewhere in the region (e.g., Campbell, 2018). A pattern of cold winters and the occasional warmer than average summer early in the 20<sup>th</sup> century has transitioned to both warmer winters and summers, with occasional short stanzas (3-4 months) of cooler temperatures.

Air temperature anomalies at the buoys (figure 20) showed a similar pattern to water temperatures, with warm anomalies trending towards cooler in late 2019, and again in late 2020. The patterns between the buoys were similar, but again offset, with anomalies lower at the Duck Flats. Again, that offset was partially because air temperatures tended to be cooler at the Duck Flats buoy (figures 3 and 4), if that offset is considered the overall pattern can be seen to be similar.

### **Surface Currents**

Surface currents at the VMT were as high as 1.5 knots and considerably smaller at the Duck Flats (figure 21), which is not surprising given the different locations. The Duck Flats buoy is deployed in shallow water near the head of Port Valdez, while the VMT buoy is deployed in deeper water over a steeply-sloped bottom mid-Port, where tidal currents will be stronger as the tides slosh back and forth.

Tide heights from station VDZA2 are routinely overlaid on the current data at both sites on the buoy websites (e.g., <http://www.pwswx.pwssc.org/VMT/VMT.html>) and there is clearly a

correlation between current direction and stage of the tide, as is to be expected given the large tidal ranges that are a feature of the region. As well as the semidiurnal (i.e., twice daily) tidal circulations there can also be longer period flows driven by winds and buoyancy currents (currents driven by freshwater entering saltwater). In order to examine those longer period motions the influence of the tidal currents must be removed. The standard method to detide a time series is to fit a series of tidal constituents to the time series (Foreman et al., 1995), as is done with water height observations from tide stations to produce tidal predictions. The tidal constituents correspond to the periods of orbital parameters of the celestial bodies (e.g., the sun and moon) that drive the tides. The model tide can then be subtracted from the observations to remove the high frequency tidal variability. This method works best with long time series (greater than 1 year) without any significant gaps (which can complicate fitting to the specific frequencies of the different components). A harmonic tidal analysis was conducted on the currents time series from both buoys with the T-Tide toolbox (Pawlowicz et al., 2002), but the resulting model fit was very poor, only explaining 33% of the variance at the VMT and 5% of the variance at the Duck Flats. The resulting model did not describe tidal currents well, with considerable remaining high frequency variability. It appears likely that the many gaps in the time series, as well as the considerable high frequency variability in surface currents (compared to the pressure or water height observations used at tide stations) gave poor results. Breaking the time series up into gap-free periods did not improve the result.

There are other methods to remove high frequency variability, including moving averages (Godin, 1972) and lowpass filters (reviewed Foreman et al., 1995), but the gaps in the time series created problems for those methods as well. Finally, the “Multiple Decimate and Interpolate” and “Peak Identification and Interpolation” methods of Gargett and Savidge (2016; GS16 hereafter) were adapted. Those methods are specifically for high frequency observations (less than hourly), such as those collected by the buoys.

The GS16 method uses successive decimations to remove high frequency variability and a peak identification method to identify the timing of the high and low tides; interpolation is then used to determine mean flows. The original GS16 method uses the Matlab ‘decimate’ function to resample the original time series at lower frequencies following filtering the data with a lowpass filter. The gaps in the buoy time series created problems with using ‘decimate’, so the more robust ‘resample’ function was used. Following GS16, the buoy time series were resampled 3 times by a factor of 2 to produce the low frequency time series. The ‘peakfinder’ peak identification function (Yoder, 2021) was then used to detect the timing of the low and high tides and the mean flow fit with a cubic spline. The residual mean flow was then averaged over each day to produce an average daily mean flow. The low and high tide peaks were not always detected by the peakfinder algorithm, and only instances where two successive low and high peaks were identified were used.

The GS16 method worked best at detecting residual mean flows when currents were highest and did not do well at the Duck Flats (where currents were usually low) and the parts of the year at the VMT when currents were at their lowest (fig. 22). Residual currents at the VMT were quite variable in 2019, and did not correspond to any wind events (fig. 7), the pattern is difficult to explain given the other observations. Residual currents in May-July 2020 were consistent with

eastward alongshore flow, which one might expect given freshwater driven currents: surface freshwater inputs are less dense than saltwater and tend to ride above saltwater for some distance before being mixed. In the northern hemisphere the Coriolis force will act upon freshwater flows and turn them to the right, which tends to create counterclockwise circulations. Prior work with drifters and current meters did show an eastward circulation along the southern shore (Gay, 2018). One might expect to see north or westward currents at the Duck Flats from the Lowe River or Valdez Glacier River, prior work with drifters and ship based current meters showed westward current along the northern margin of Port Valdez (Gay, 2018) but there were no periods of mean flow that corresponded to outflows at either river, despite both hydrographs showing several outflow events that may have been caused by precipitation events or glacial outburst floods (figure 23). Surface currents in Port Valdez are also strongly influenced by winds (Gay, 2018) and untangling wind and tidal effects without a more elaborate tidal model may not be possible.

In order to examine how the timing of currents at the two buoys varied compared to the water height observations at the VDZA2 tide station, a cross covariance analysis was done. The covariance between two quantities measures how much in concert the quantities change (i.e., “if one goes up how much does the other go up” and vice versa). In a cross covariance analysis the covariance between the quantities is examined at several different times to see if one lags or leads the other. The results of the cross covariance analysis showed that the surface currents at the buoys tended to lag the tidal height by about 45 minutes (figure 24). In other words, slack currents occurred about 45 minutes after the time of the high and low tides.

## Conclusions

The analysis done here shows the patterns one would expect of meteorological and oceanographic observations in a subarctic region with a large tidal range. The main observations may be summarized as follows:

- Air and water temperatures, and solar radiation followed a seasonal sinusoid with maxima in August and minima in February. Temperatures were slightly cooler at the Duck Flats buoy than at the VMT buoy.
- Relative humidity was high at both sites and followed the seasonal temperature pattern.
- Air pressure was similar between both sites and driven by large scale atmospheric circulations.
- Winds were mostly from the east in autumn and winter, transitioning to weak easterly and stronger westerly sea breezes during the summer months.
- Wave directions tended to match wind directions. The highest waves were observed during autumn/winter storms and spring/summer sea breeze generated waves were on order of one foot.
- A temperature climatology was constructed that shows a persistent warming pattern over the past 112 years.
- Air and water temperatures at the buoy sites were warmer than average in 2019 and tended towards cooler than average in 2020, likely reflecting large scale climate fluctuations.
- Surface currents had a tidal component, but several attempts to remove the high frequency tidal variability to examine circulation patterns did not produce useful results, likely due to gaps in the time series and non-tidal variability (e.g., winds). Currents at the Duck Flats buoy were much weaker than at the VMT buoy.

- Cross covariance analysis comparing the timing of currents at the buoys compared to the tides at the Port Valdez tide station showed that surface currents tended to lag the tides by approximately 45 minutes.

## Literature cited

- Amaya, D.J., Miller, A.J., Xie, S-P. and Y. Kosaka. 2020. Physical drivers of the summer 2019 North Pacific marine heatwave. *Nature Communications*. 11, 1903. doi: 10.1038/s41467-020-15820-w
- Campbell, R.W. 2018. Hydrographic trends in Prince William Sound, Alaska, 1960–2016. *Deep-Sea Res II*. doi:10.1016/j.dsr2.2017.08.014
- Foreman, M.G.G., Crawford, W.R. and R.F. Marsden. 1995. De-tiding: Theory and practice. pp. 203-239 *in*: Quantitative Skill Assessment for Coastal Ocean Models. American Geophysical Union. doi: 10.1029/CE047p0203
- Gargett, A.E. and D. Savidge. 2016. Separation of Short Time Series of Currents into “Fluctuations”, “Tides” and “Mean” Flow. *Journal of Atmospheric and Ocean Technology*. doi: 10.1175/JTECH-D-15-0232.1
- Gay, S.M. 2018. Circulation in Port Valdez, Alaska measured by Lagrangian Drifter Experiments, towed acoustic Doppler current profiler and hydrographic profiles in June and September 2016, and March 2017. PWSRCAC report # 700.431.180322.PtVdzCirculation
- Godin, G. 1972. The analysis of tides. University of Toronto Press. 264pp
- Papineau, J.M. 2001. Wintertime temperature anomalies in Alaska correlated with ENSO and PDO. *International Journal of Climatology* 21:1577 – 1592 doi:10.1002/joc.686
- Pawlowicz, R., Beardsley, B. and S. Lentz. 2002. Classical tidal harmonic analysis including error estimates in MATLAB using T\_TIDE. *Computers and Geosciences* 28:929-937 doi: 10.1016/S0098-3004(02)00013-4
- Lethcoe, J. and N. Lethcoe. 2009. *Crusing guide to Prince William Sound (5<sup>th</sup> ed.)*. Prince William Sound Books, Valdez. 202 pp
- Newman, M., Alexander, M. A., Ault, T., Cobb, K. M., Deser, C., Di Lorenzo, E., Mantua, N. J., Miller, A.J., Minobe, S., Nakamura, H., Schneider, N., Vimont, D., Phillips, A., Smith, C. A. and J.D. Scott. 2016. The Pacific Decadal Oscillation, Revisited. *Journal of Climate* 29, 12; doi:10.1175/JCLI-D-15-0508.1
- NOAA/NWS NCEP Climate Prediction Center. 2020. El Niño/southern oscillation (ENSO) diagnostic discussion, 10 December 2020 [https://www.cpc.ncep.noaa.gov/products/analysis\\_monitoring/enso\\_disc\\_dec2020/ensodisc.pdf](https://www.cpc.ncep.noaa.gov/products/analysis_monitoring/enso_disc_dec2020/ensodisc.pdf)
- Yoder, N. 2021. peakfinder(x0, sel, thresh, extrema, includeEndpoints, interpolate) (<https://www.mathworks.com/matlabcentral/fileexchange/25500-peakfinder-x0-sel-thresh-extrema-includeendpoints-interpolate>), MATLAB Central File Exchange. Retrieved March 26, 2021



## Figures



Figure 1: Satellite photo of Port Valdez showing the location of the two buoys.



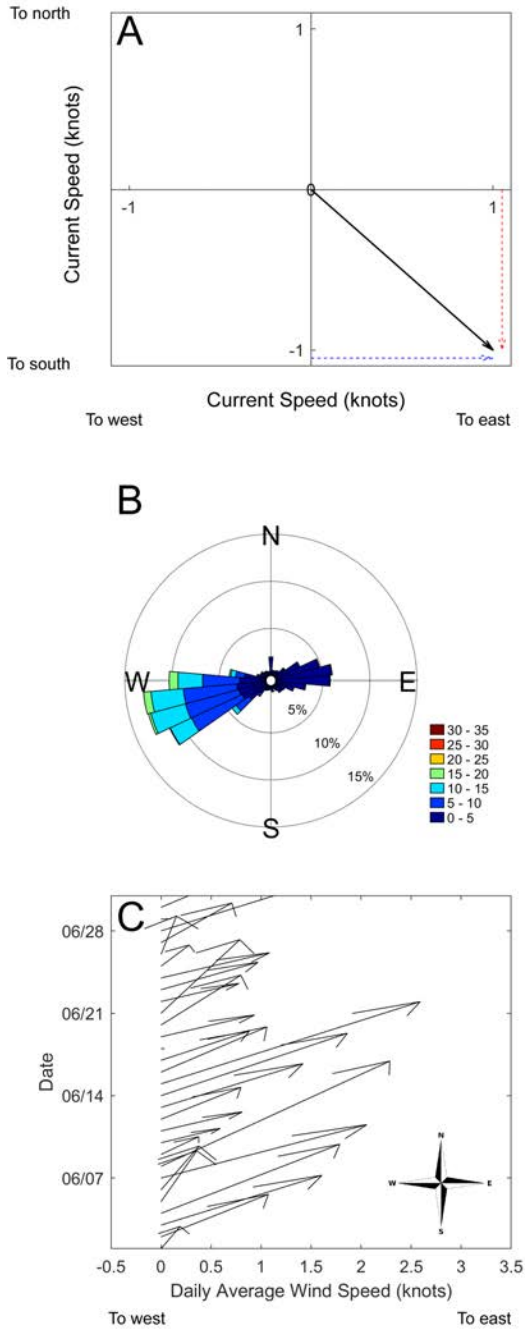


Figure 2: Examples of the visualization of vector data. Panel A shows an example of a vector observation, for example a 1 knot current to the southeast. The vector may be broken up into two components, an east-west component (blue arrow) and a north-south component (red arrow). Panel B: An example wind rose summarizing wind observations made in June 2020. The bars indicate 10-degree bands of wind directions (direction from), the lengths of the bars indicate frequency (how often winds in each band were observed) and the color encodes wind speeds. Panel C: An example of a quiver plot, showing daily average wind vectors (direction in which the air is traveling) for June 2020. The angle of the arrow indicates the direction on the compass rose and the length of the arrow indicates average wind speed, scaled to match the bottom axis.

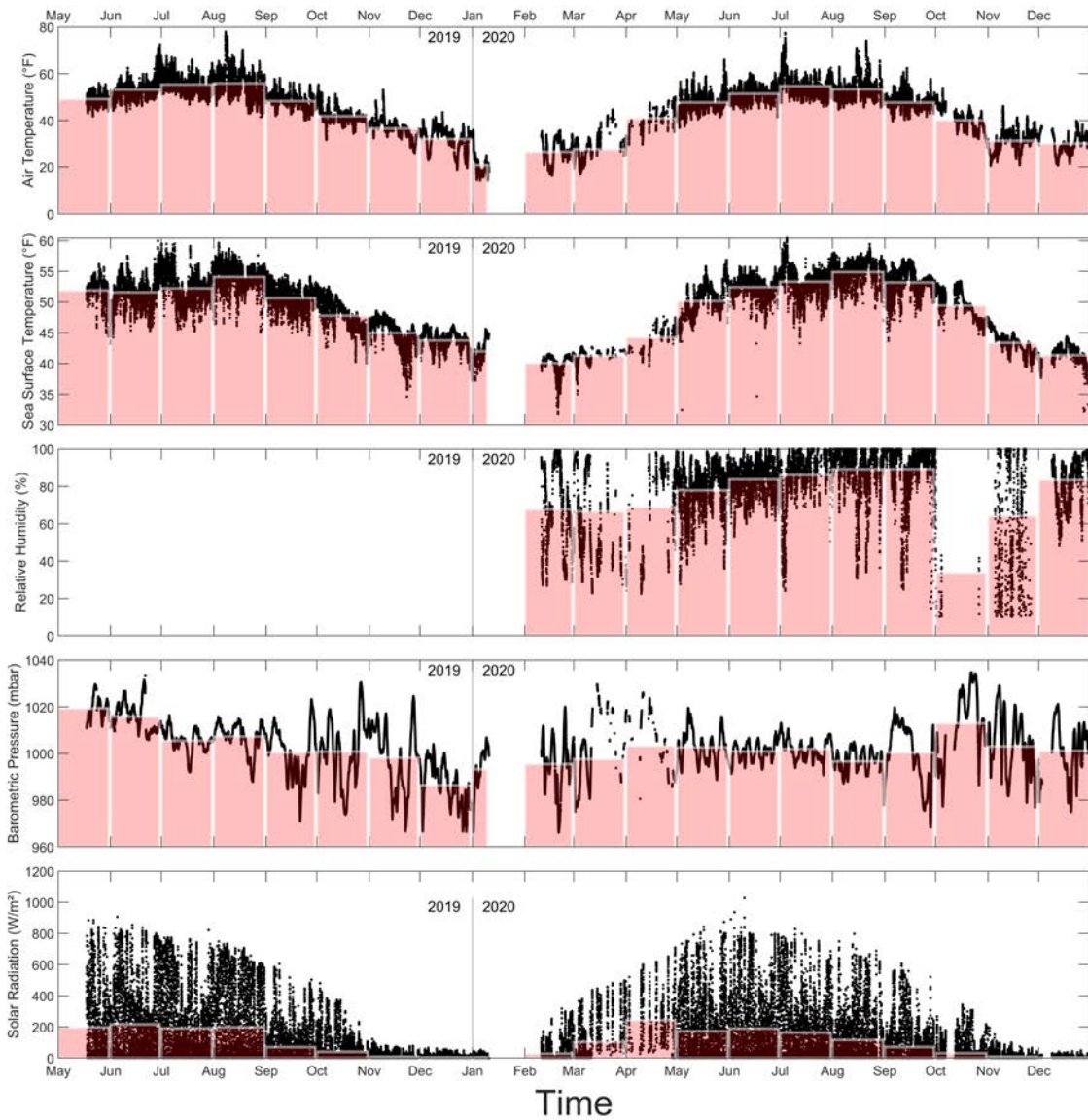


Figure 3: Scalar observations at the VMT buoy, including air (top panel) and water (2<sup>nd</sup> panel) temperatures, relative humidity (3<sup>rd</sup> panel), barometric pressure (4<sup>th</sup> panel) and solar radiation (bottom panel). Black dots are observations, bars indicate monthly averages.

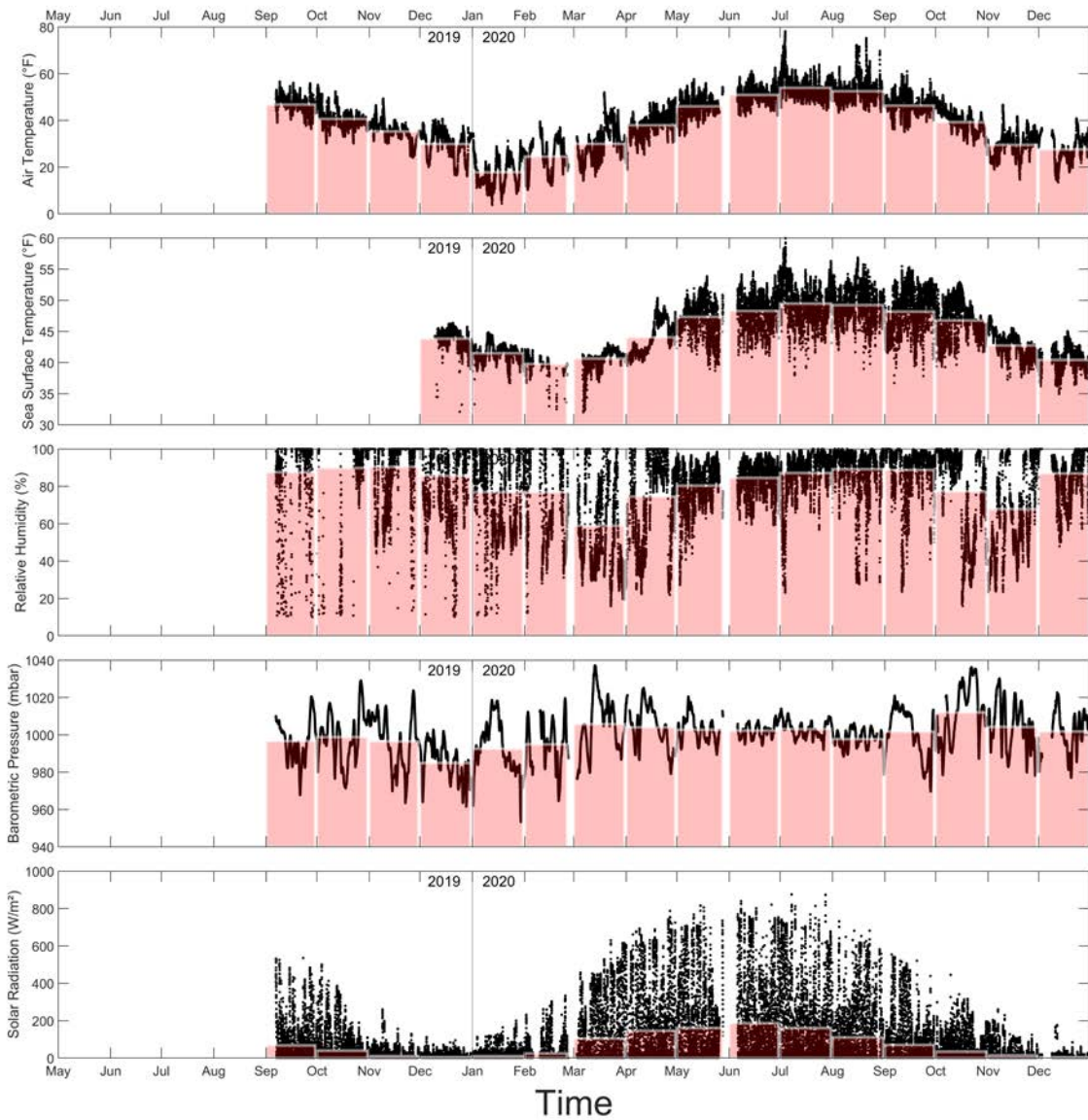


Figure 4: Scalar observations at the Duck Flats buoy, including air (top panel) and water (2<sup>nd</sup> panel) temperatures, relative humidity (3<sup>rd</sup> panel), barometric pressure (4<sup>th</sup> panel) and solar radiation (bottom panel). Black dots are observations, bars indicate monthly averages.

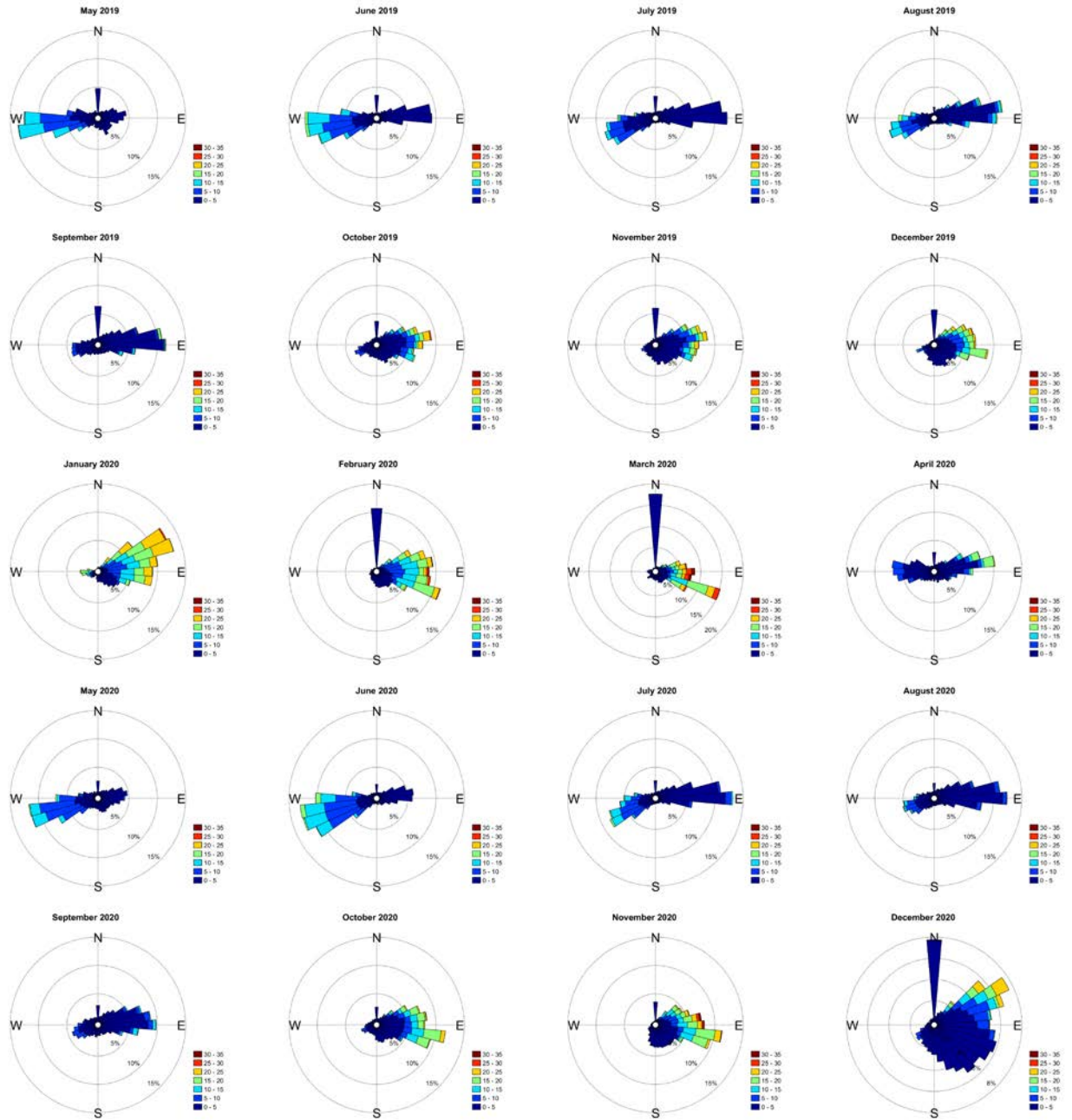


Figure 5: Monthly wind roses at the VMT buoy. Bars indicate the direction from and the color scale indicates wind velocities. Color scale is equivalent among the figures (i.e., all the figures are directly comparable).



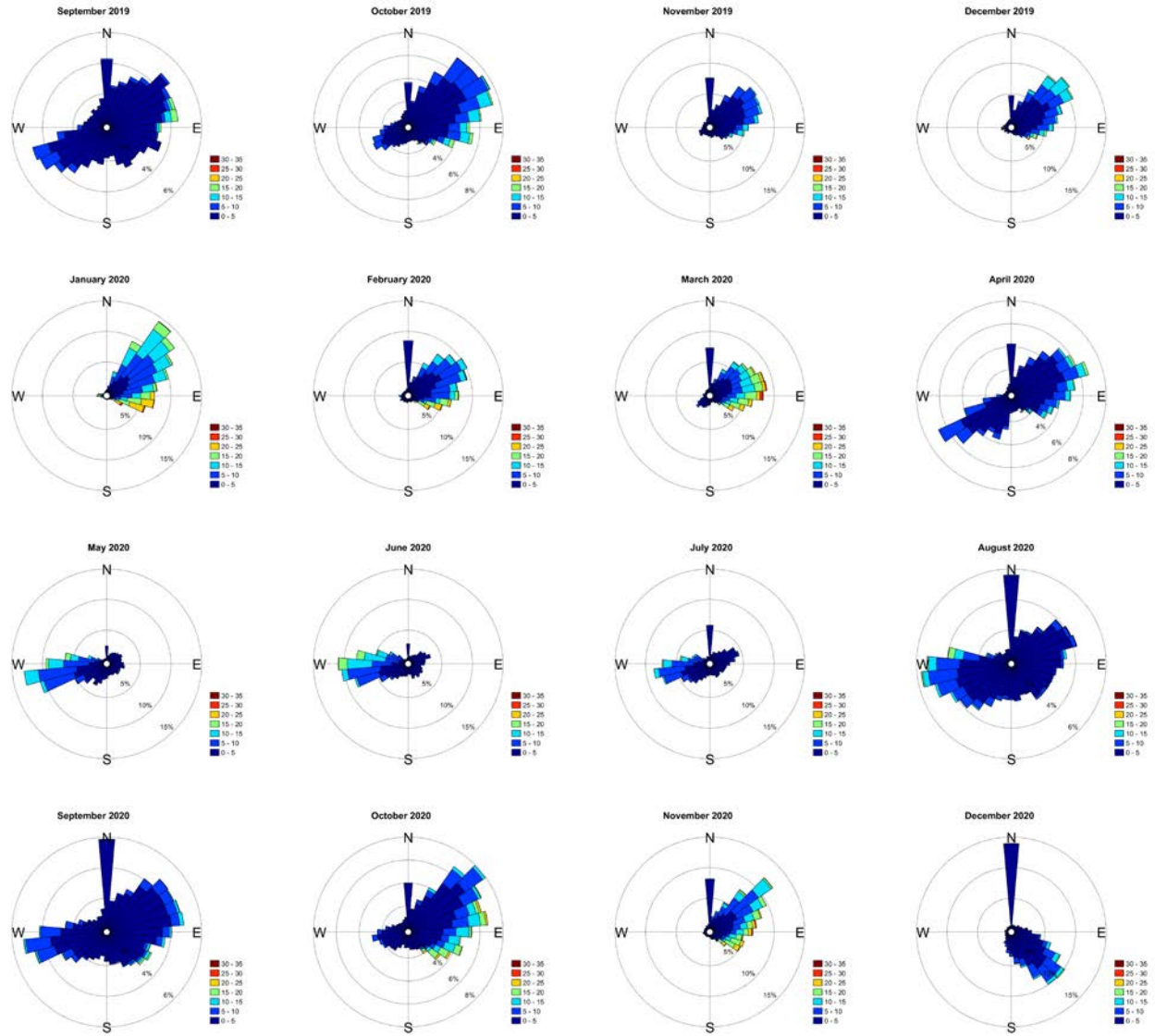


Figure 6: Monthly wind roses at the Duck Flats buoy. Bars indicate the direction from and the color scale indicates wind velocities. Color scale is equivalent among the figures (i.e., all the figures are directly comparable).

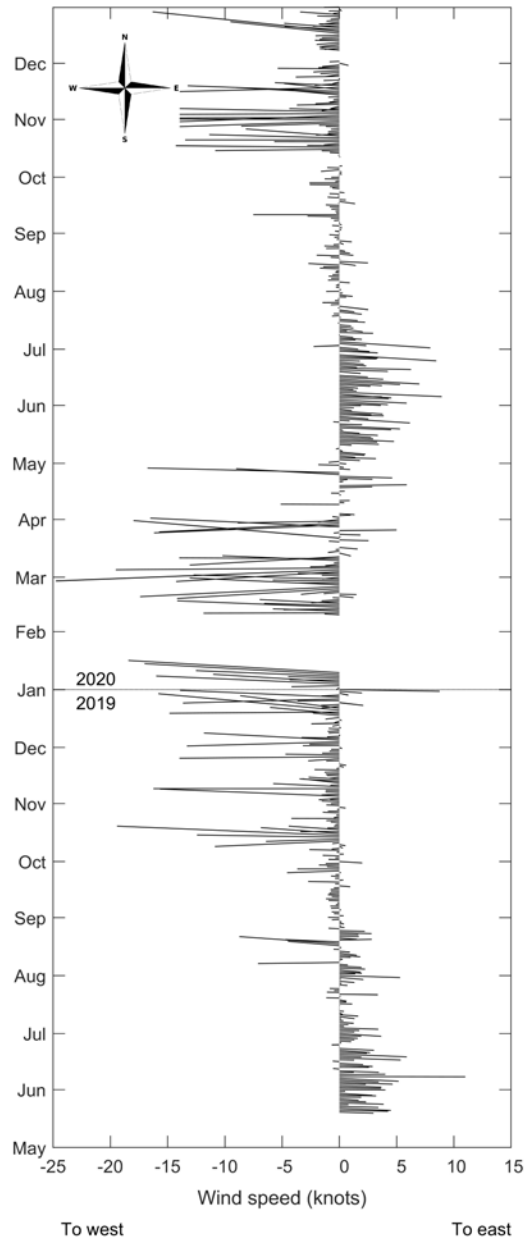


Figure 7: Quiver plot of average daily wind vectors at the VMT buoy. The length of each stick indicates wind speed and the angle indicates the direction from.



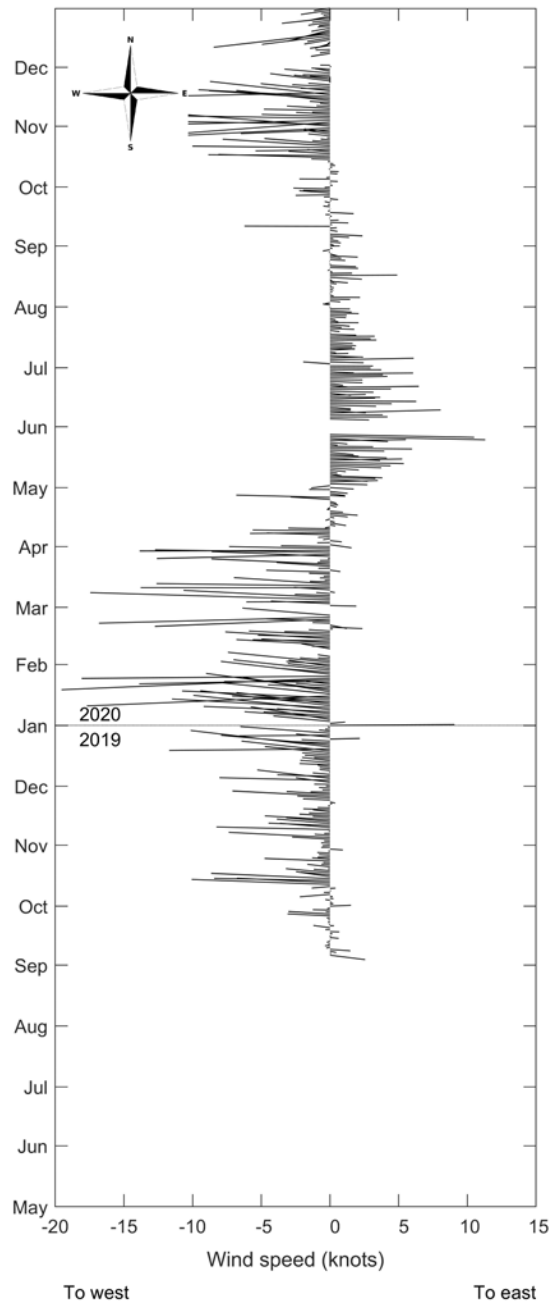


Figure 8: Quiver plot of average daily wind vectors at the Duck Flats buoy. The length of each stick indicates wind speed and the angle indicates the direction from.

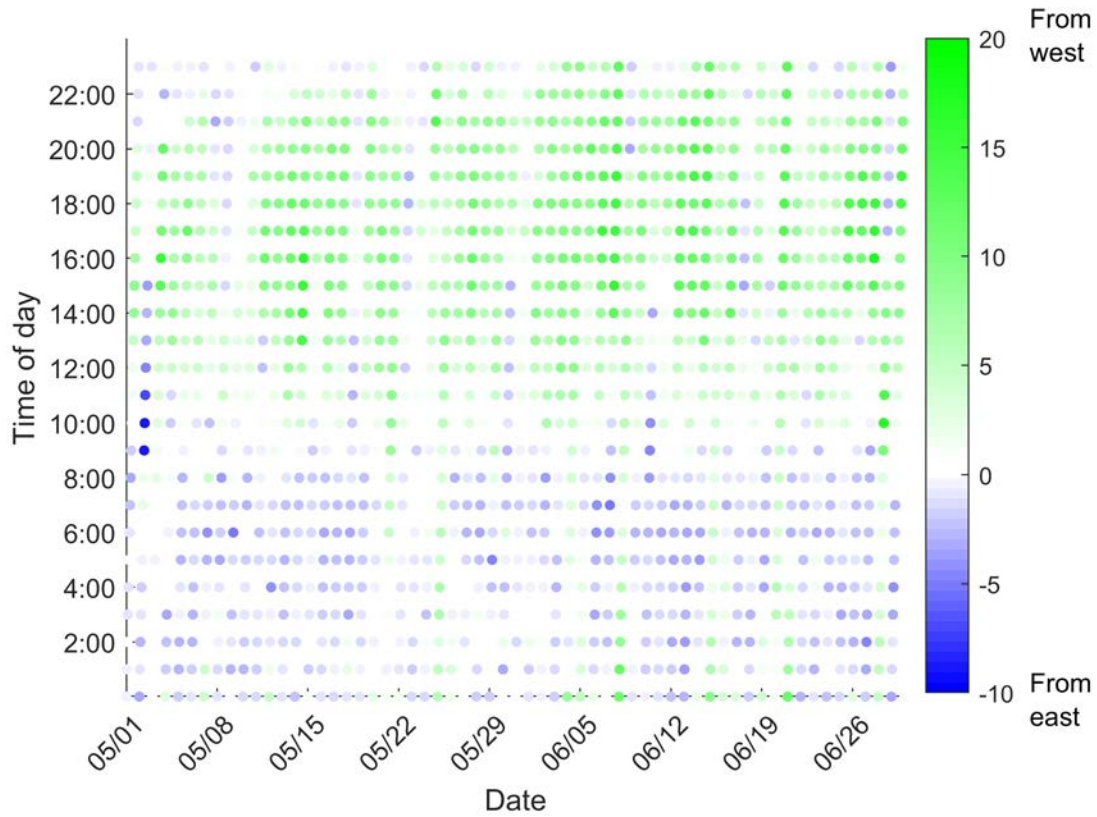


Figure 9: Daily east-west sea breezes at the VMT buoy in May-June 2020. Only the east-west component of the winds are shown. Green colors scale with the strength westerly winds and blue color scale with the strength of easterly winds.

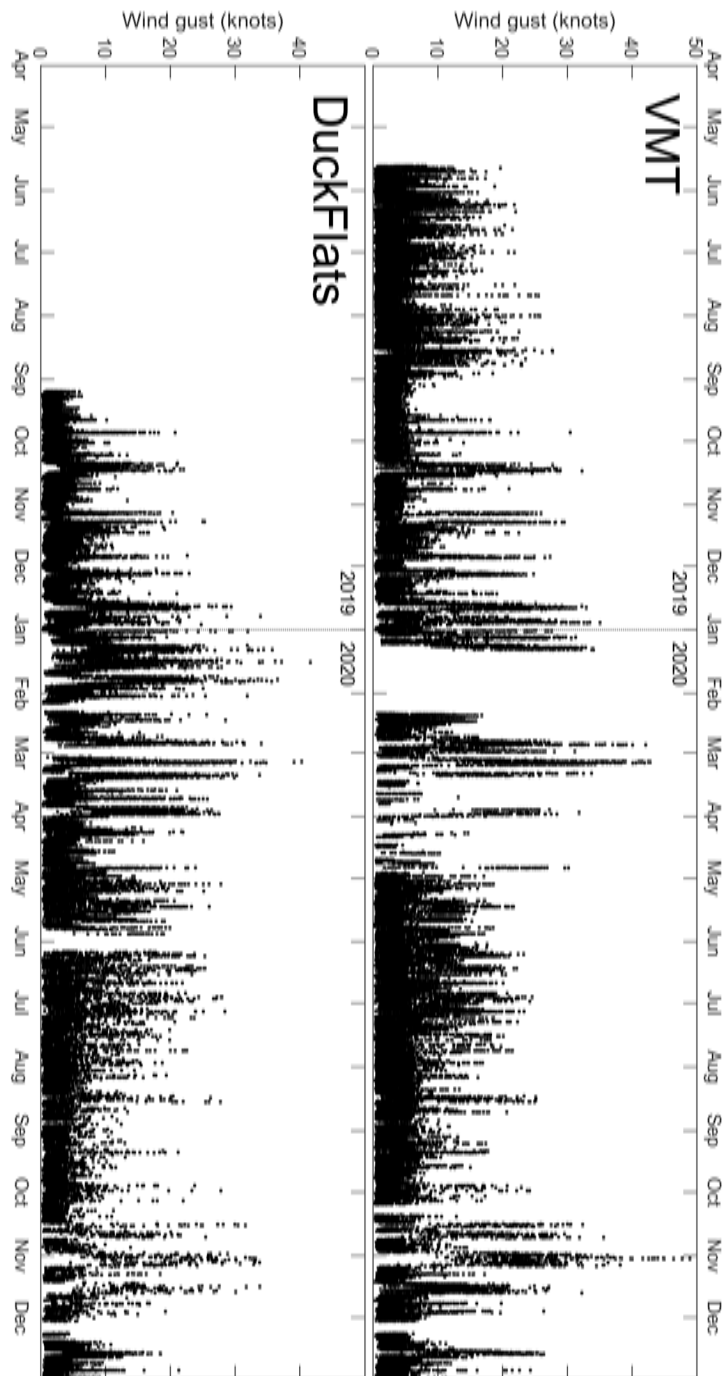


Figure 10: Wind gust time series at the VMT (top panel) and Duck Flats (bottom panel).

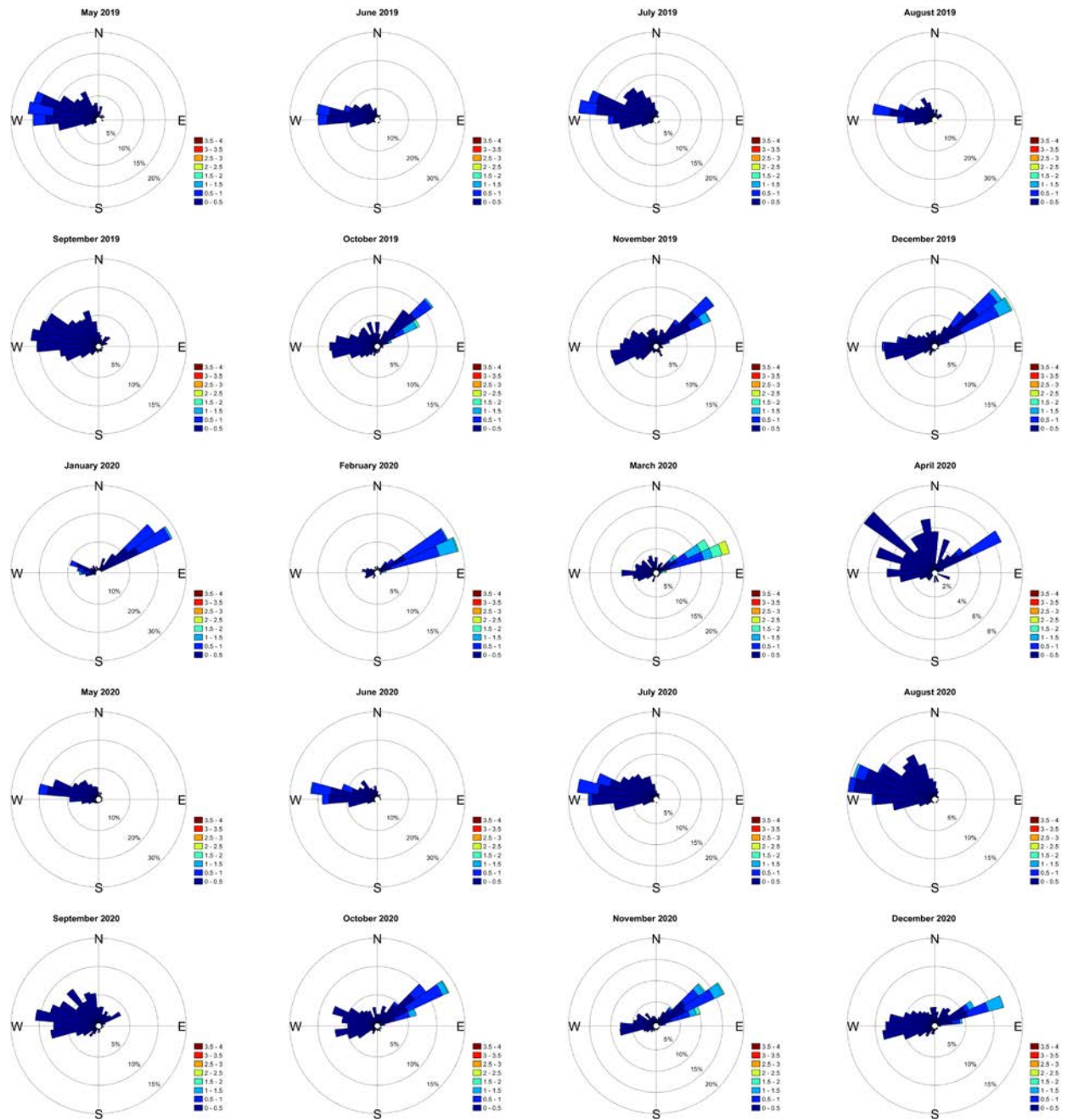


Figure 11: Monthly wave roses at the VMT buoy. Bars indicate the direction to and the color scale indicates significant wave heights. Color scale is equivalent among the figures (i.e., all the figures are directly comparable).

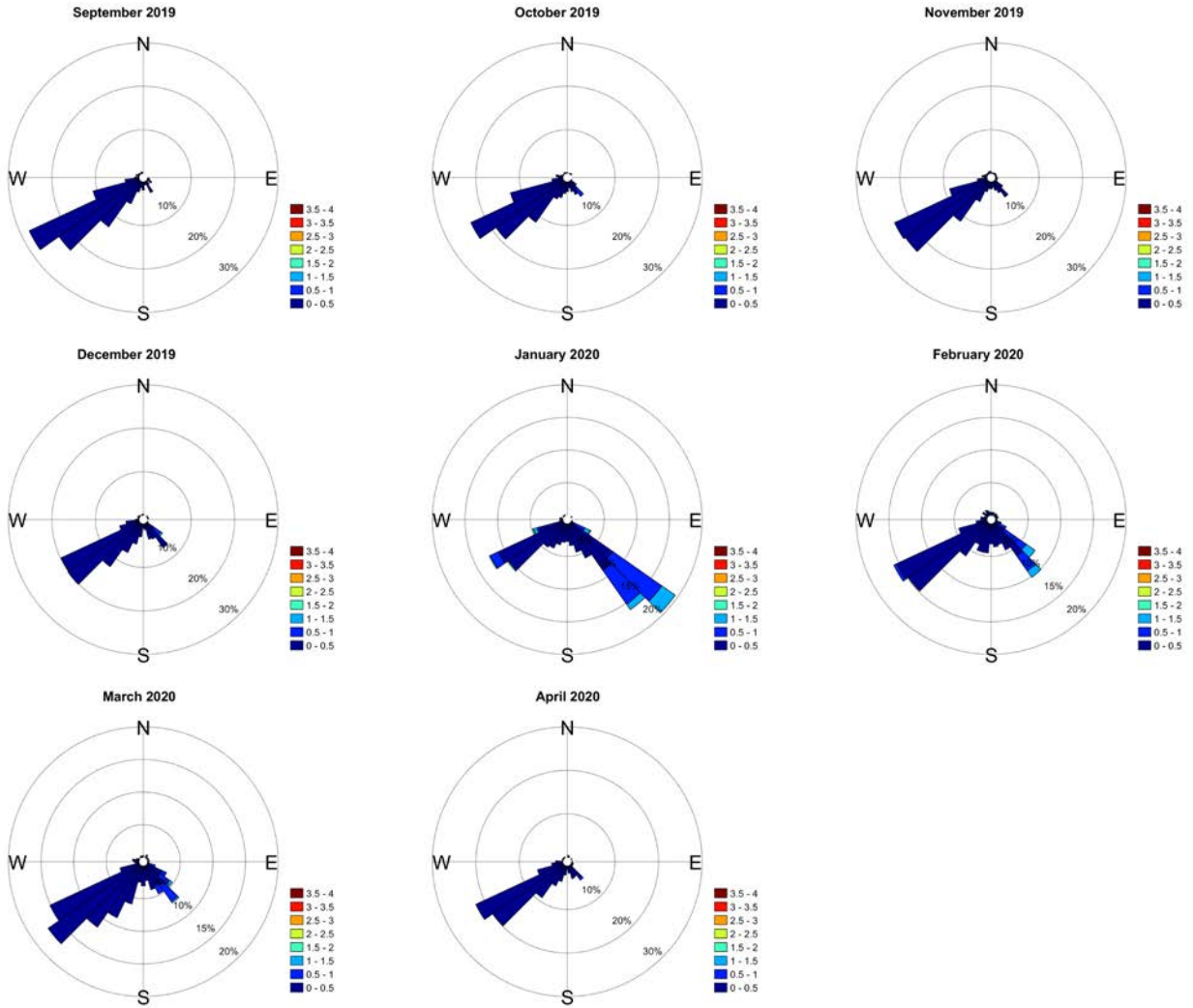


Figure 12: Monthly wave roses at the Duck Flats buoy. Bars indicate the direction to and the color scale indicates significant wave heights. Color scale is equivalent among the figures (i.e., all the figures are directly comparable).

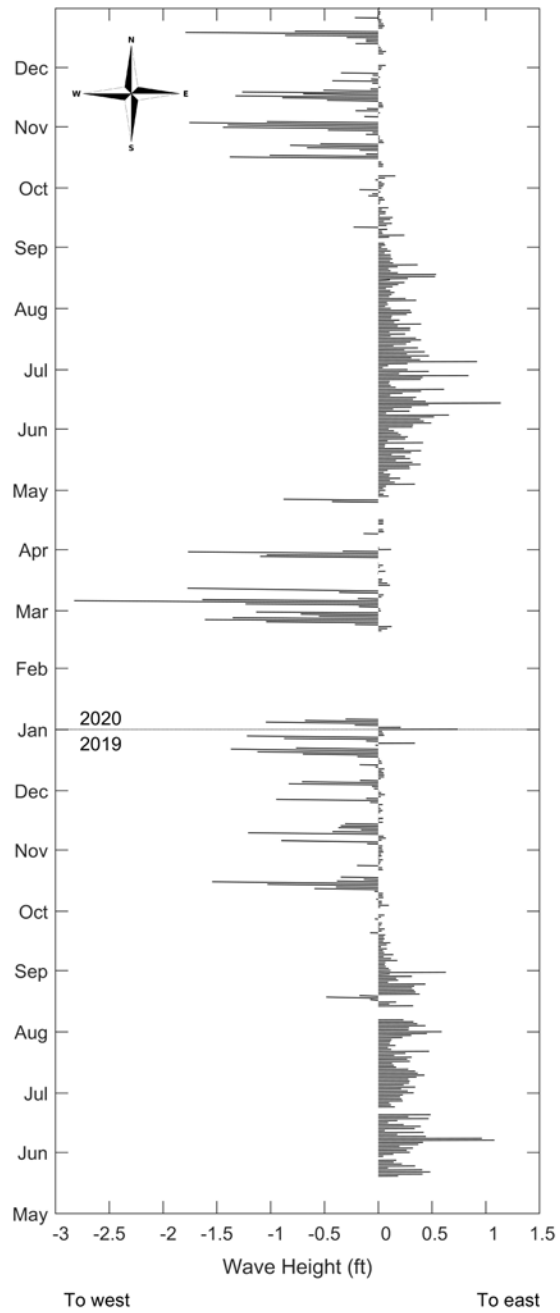


Figure 13: Quiver plot of average daily wave vectors at the VMT buoy. The length of each stick indicates wave height and the angle indicates the direction to.



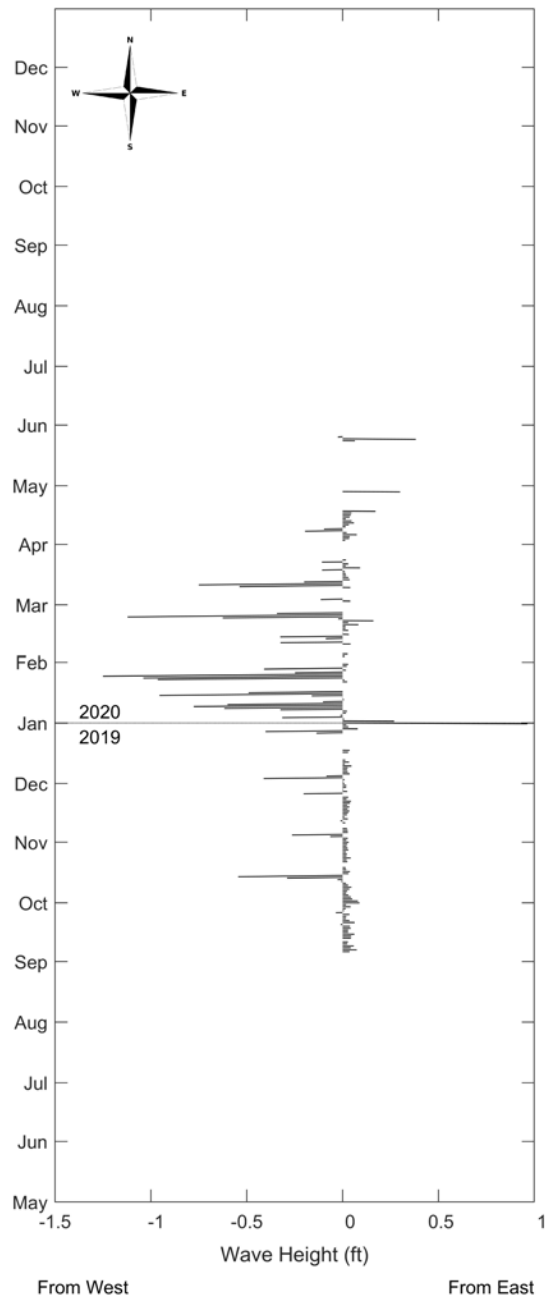


Figure 14: Quiver plot of average daily wave vectors at the Duck Flats buoy. The length of each stick indicates wave height and the angle indicates the direction to.

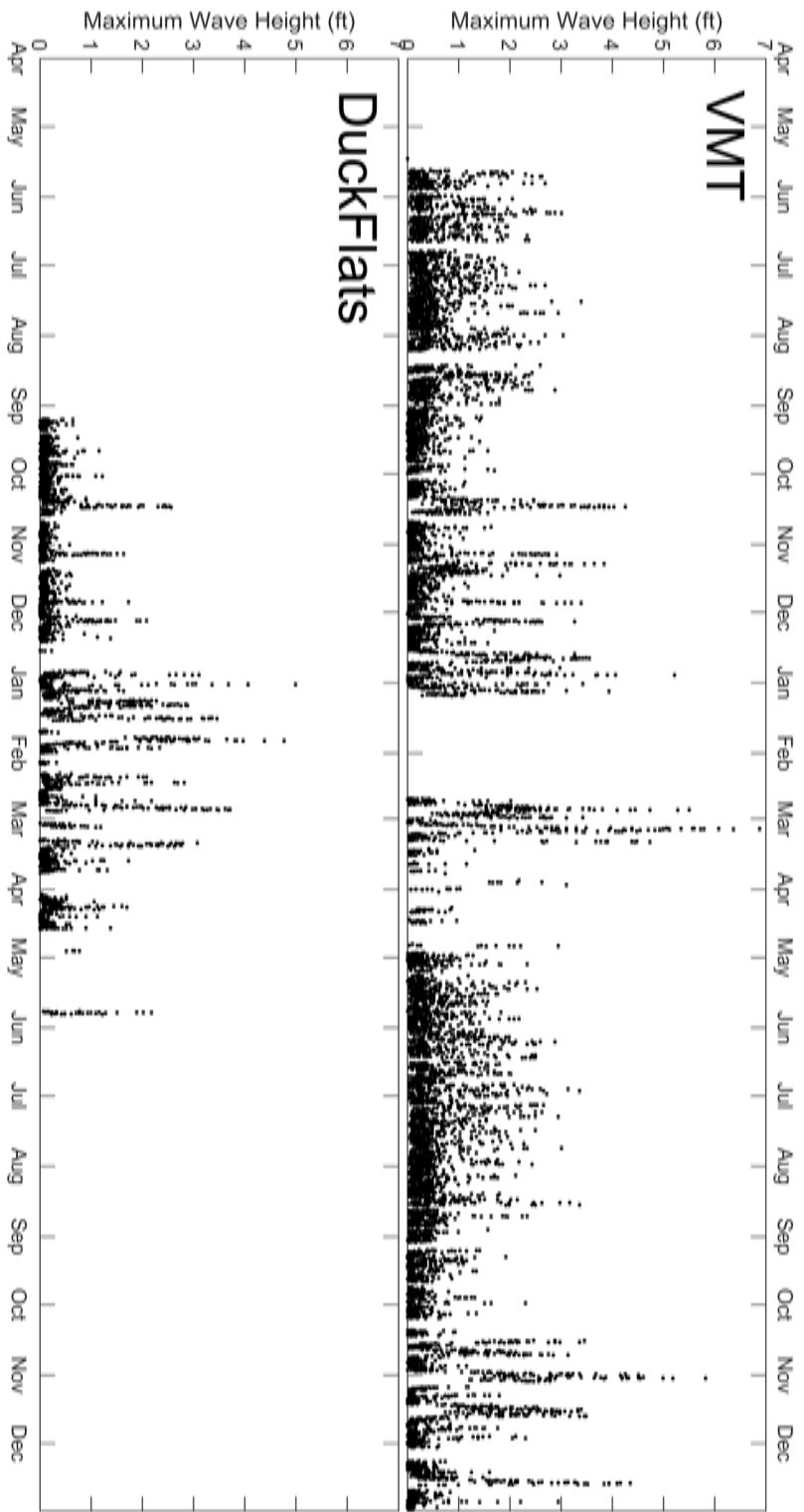


Figure 15: Time series of maximum wave heights observed at the VMT (top panel) and Duck Flats (bottom panel) buoys.

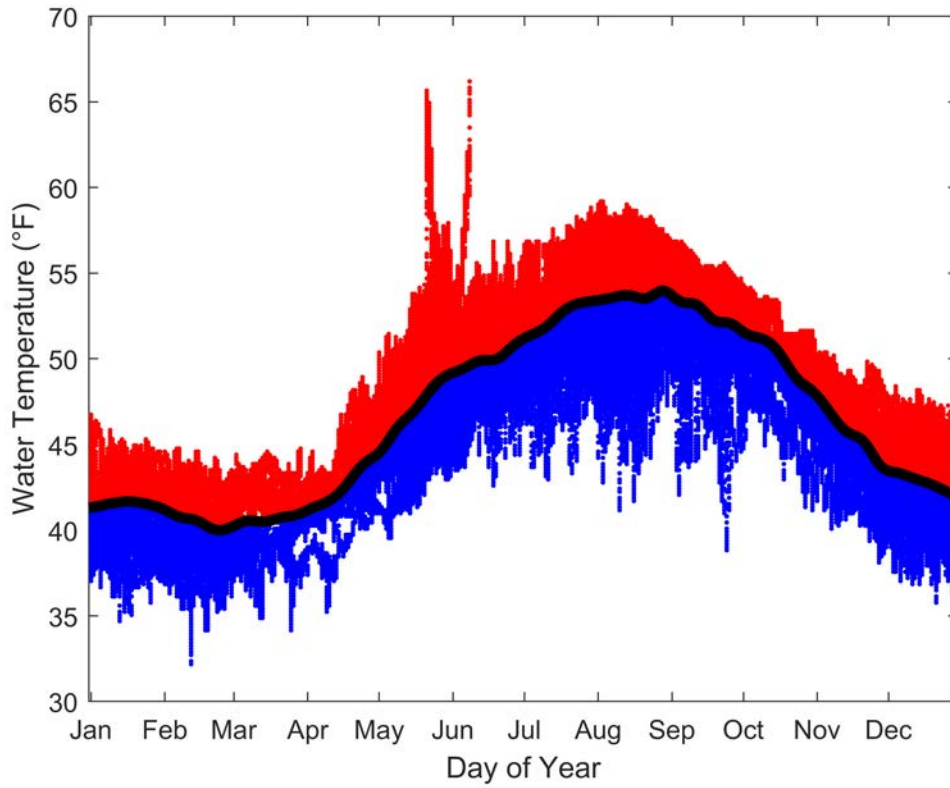


Figure 16: Annual average temperature cycle at the NOAA tide station VDZA2 in Valdez harbor. Air temperature data was overlaid from all years (2009-present) by day of year. Dots (red and blue) indicate observations and the black line indicates the weekly average.

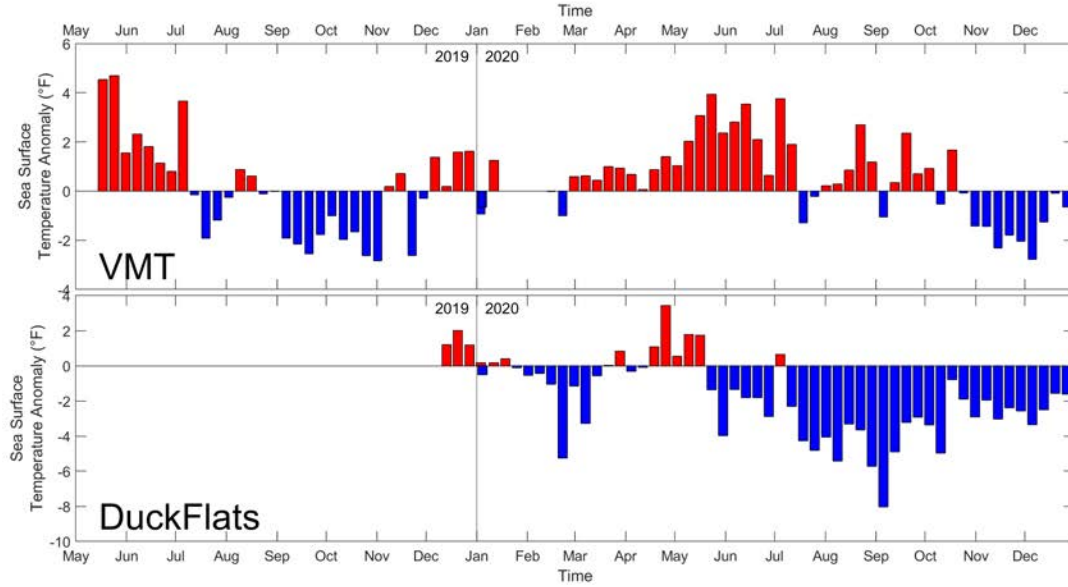


Figure 17: Weekly sea surface temperature anomalies at the VMT (top panel) and Duck Flats (bottom panel) buoys. Anomalies are the departure of weekly average temperatures from the weekly average at the VDZA2 tide station.

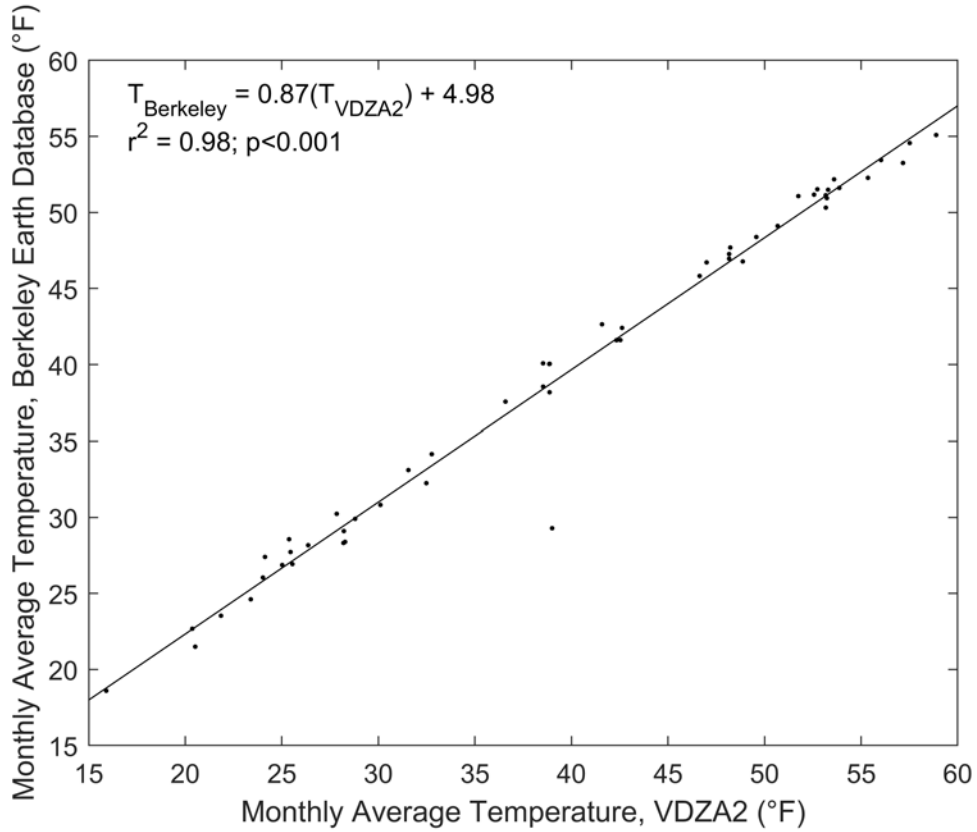


Figure 18: Comparison of monthly average air temperature estimates from the Berkeley Earth database and monthly average temperatures calculated at the VDZA2 station on months where the two time series overlapped (2009-2013). The regression line was fit by least squares.

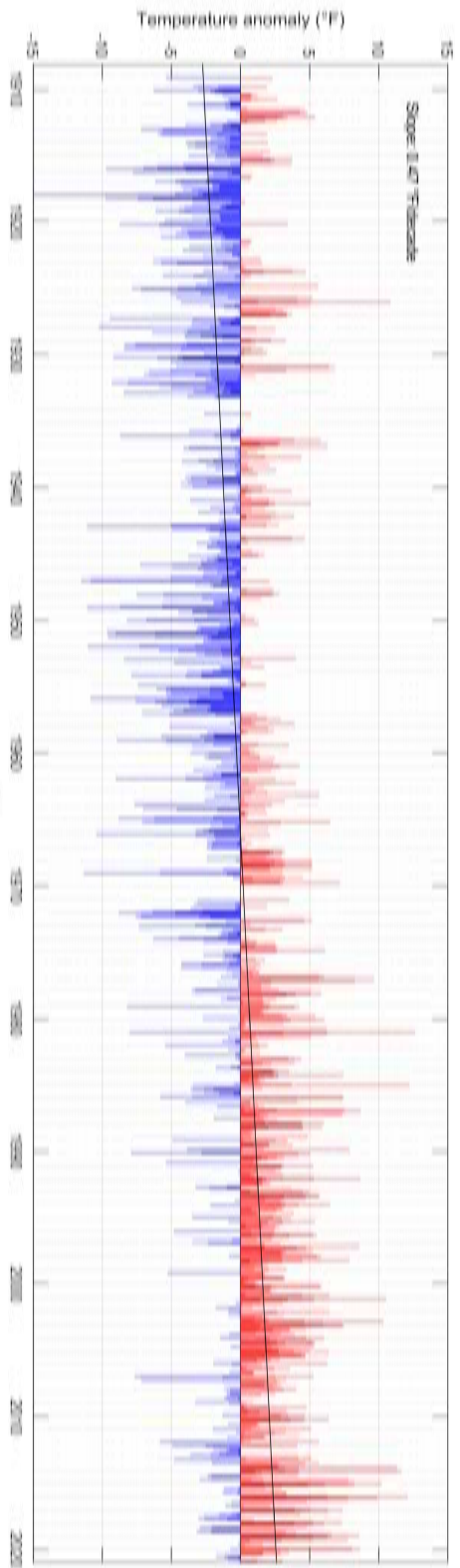


Figure 19: Air temperature anomalies from the combined Berkeley Earth database/VDZA2 monthly temperature estimates, 1908 - 2020.



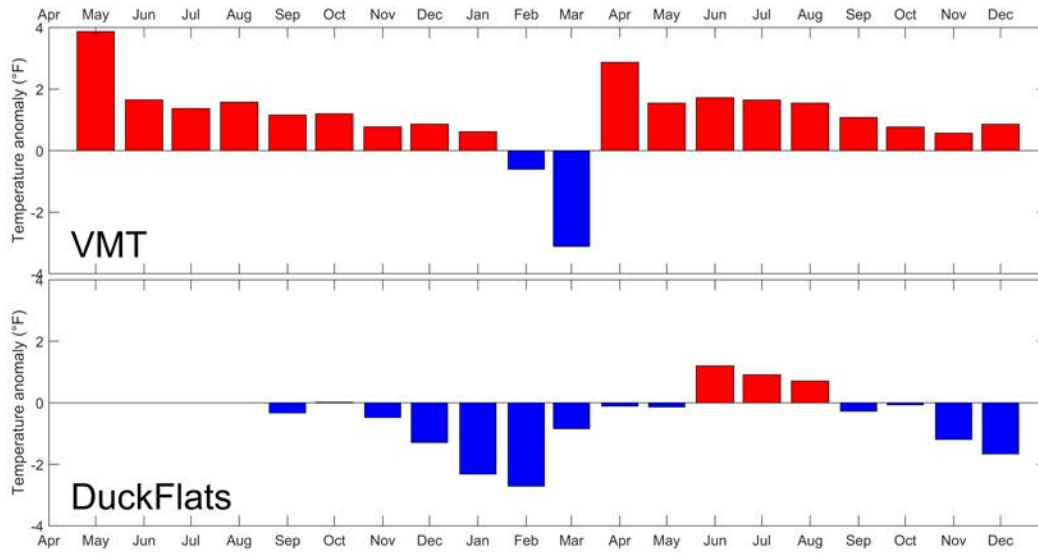


Figure 20: Monthly average air temperature anomalies at the VMT (top panel) and Duck Flats (bottom panel) buoys using the Berkeley Earth/VDZA2 climatology.

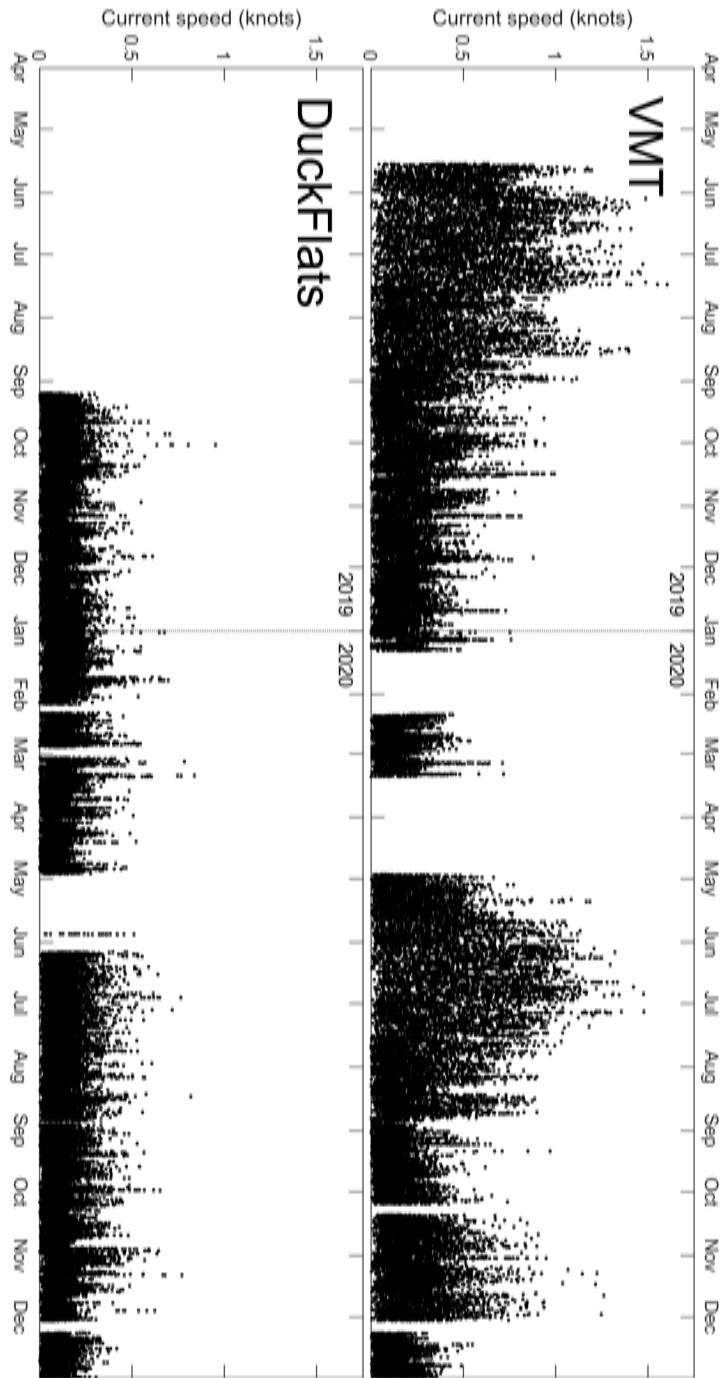


Figure 21: Current speed time series at the VMT (top panel) and Duck Flats (bottom panel).

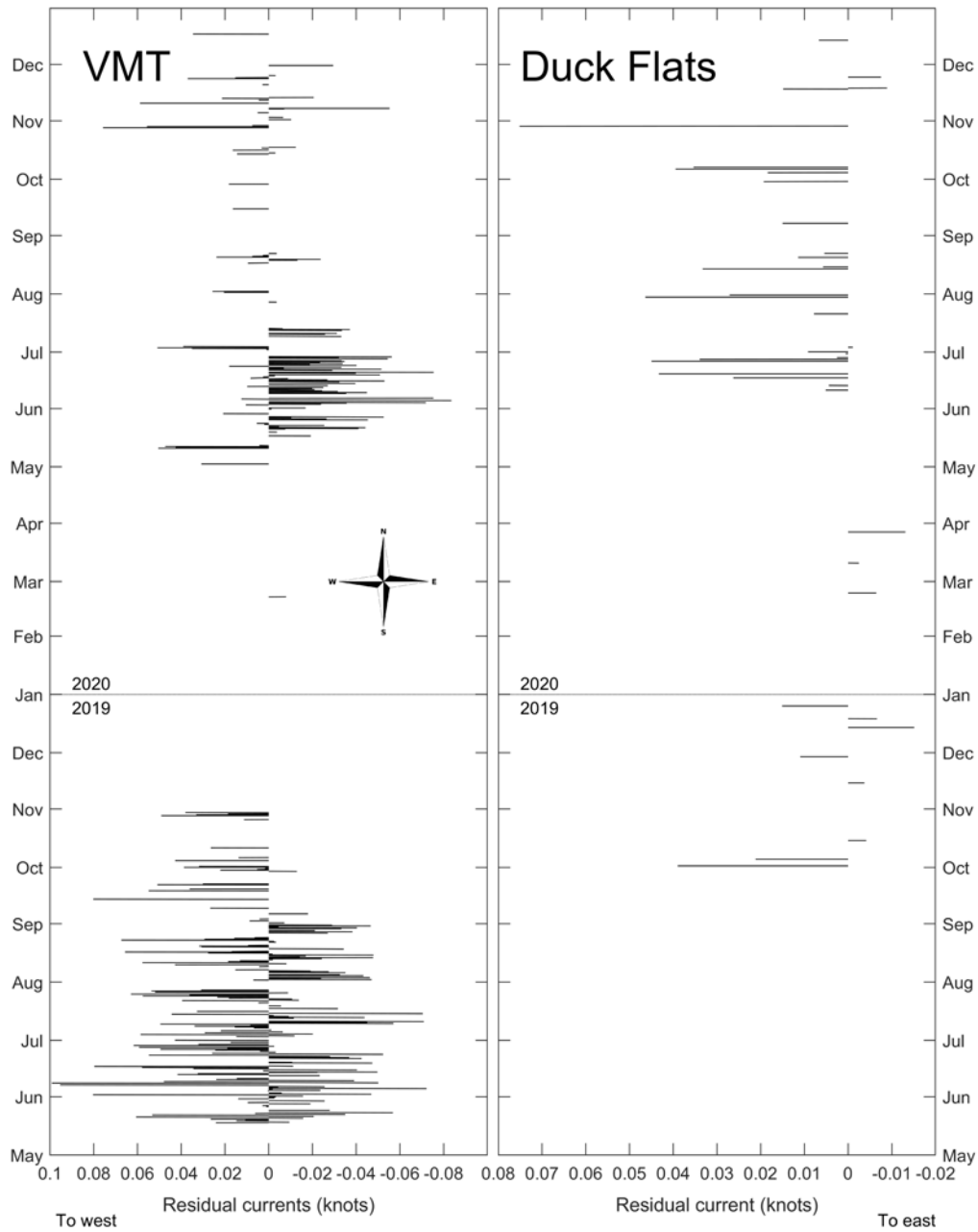


Figure 22: Quiver plot of residual mean flow (residual currents after tidal effects were removed - see text). Length of the sticks indicate velocity and angle of the stick indicates direction to.

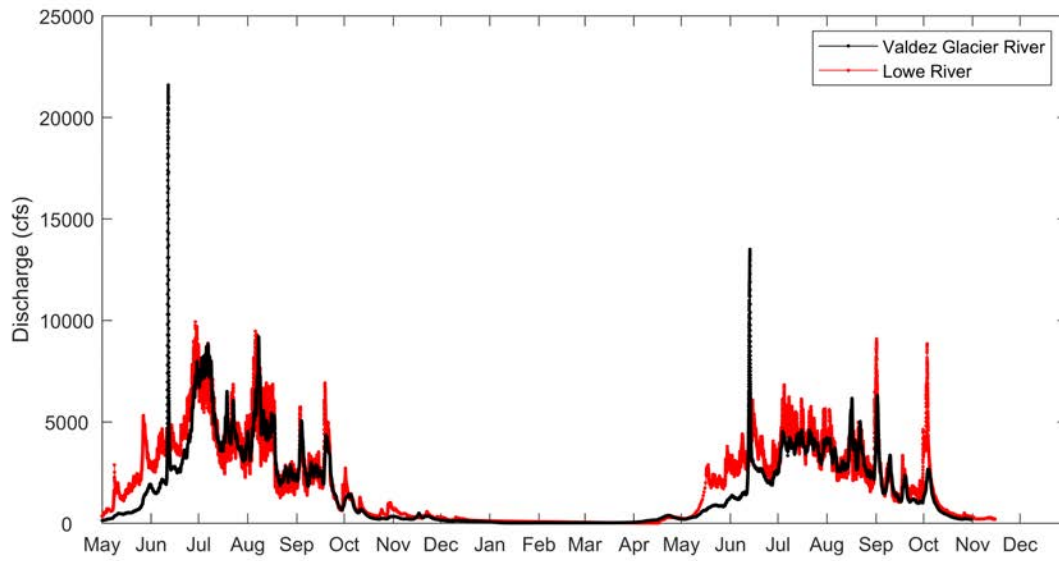


Figure 23: Hydrograph of discharge at the Lowe River (USGS station 15226620) and Valdez Glacier River (USGS station 15227090). Discharge data was downloaded from [waterdata.usgs.gov](http://waterdata.usgs.gov).

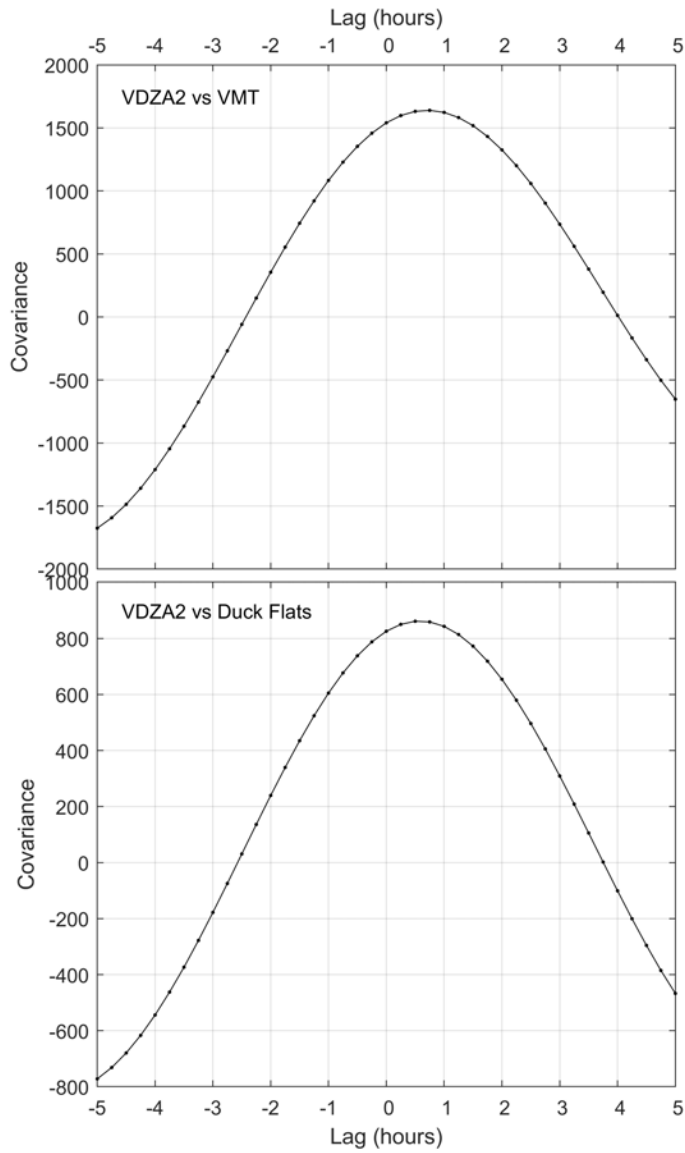


Figure 24: Cross covariance between tidal currents at the VMT (top panel) and Duck Flats (bottom panel) buoys and water heights at station VDZA2. Lags are relative to the time at VDZA2.

**Appendix 1: Table of averages and minimum/maximum values at the VMT buoy, by month.**

Month	Air Temperature (°F)	Water Temperature (°F)	Relative Humidity (%)	Barometric Pressure (%)	Solar Radiation (W/m <sup>2</sup> )	Wind Speed (knots)	Wind Gust (knots)	Significant Wave Height (ft)	Maximum Wave Height (ft)	Current Speed (knots)
January	21.00	41.72	79.03	991.72	4.39	8.78	20.36	0.52	0.94	0.18
	13.91 - 35.88	33.86 - 45.64	62.93 - 98.00	966.18 - 1007.21	0.00 - 53.30	0.00 - 26.63	0.00 - 66.17	0.00 - 2.08	0.00 - 3.94	0.00 - 0.76
February	26.61	40.08	67.70	995.48	28.67	7.61	13.93	0.82	1.44	0.15
	16.48 - 35.77	31.75 - 41.78	26.78 - 99.50	966.15 - 1020.00	0.00 - 317.39	0.00 - 34.77	0.00 - 81.85	0.00 - 3.26	0.00 - 5.50	0.00 - 0.54
March	27.70	41.27	66.56	997.59	103.11	7.88	16.94	0.70	1.22	0.14
	16.99 - 44.64	35.00 - 42.80	22.86 - 98.50	975.08 - 1029.62	0.00 - 497.85	0.00 - 34.77	0.00 - 83.18	0.00 - 3.78	0.00 - 6.88	0.00 - 0.72
April	40.92	44.24	68.98	1003.30	243.49	3.42	9.11	0.21	0.42	0.20
	29.30 - 50.07	39.61 - 47.64	22.55 - 98.70	980.56 - 1026.09	0.00 - 709.01	0.00 - 21.83	0.00 - 58.66	0.00 - 1.34	0.00 - 2.94	0.01 - 0.66
May	48.16	50.71	77.92	1007.92	180.08	3.90	8.32	0.25	0.49	0.35
	36.80 - 65.95	32.38 - 56.86	27.63 - 98.70	988.68 - 1029.65	0.00 - 885.68	0.00 - 18.02	0.00 - 42.16	0.00 - 1.47	0.00 - 2.69	0.00 - 1.20
June	52.32	52.01	83.74	1008.29	203.22	4.79	9.70	0.35	0.66	0.51
	41.35 - 72.50	34.67 - 59.99	53.15 - 100.00	991.38 - 1033.57	0.00 - 1027.90	0.00 - 19.90	0.00 - 47.76	0.00 - 1.86	0.03 - 3.36	0.00 - 1.49
July	55.04	52.78	86.08	1003.74	177.40	3.41	7.50	0.30	0.57	0.40
	45.95 - 77.36	43.27 - 60.44	24.08 - 100.00	990.72 - 1016.45	0.00 - 828.67	0.00 - 21.23	0.00 - 49.66	0.00 - 1.73	0.03 - 3.39	0.00 - 1.61
August	54.64	54.48	89.23	1002.07	158.09	3.79	8.77	0.29	0.55	0.31
	41.47 - 77.86	45.06 - 59.65	30.71 - 100.00	977.82 - 1015.77	0.00 - 797.59	0.00 - 22.66	0.00 - 53.90	0.00 - 2.08	0.03 - 3.36	0.00 - 1.40
September	47.97	51.92	89.28	1000.47	70.72	2.56	5.64	0.11	0.23	0.19
	39.56 - 62.37	43.67 - 57.07	14.78 - 100.00	968.33 - 1023.27	0.00 - 606.41	0.00 - 21.28	0.00 - 59.19	0.00 - 0.96	0.00 - 2.30	0.00 - 0.97
October	41.05	48.54	33.91	1006.34	36.49	4.71	10.34	0.29	0.54	0.24
	28.14 - 55.35	40.02 - 53.44	10.22 - 93.30	973.84 - 1034.70	0.00 - 480.61	0.00 - 28.59	0.00 - 70.35	0.00 - 2.59	0.00 - 4.51	0.00 - 1.00
November	33.91	44.18	64.25	1000.61	8.67	5.58	10.73	0.38	0.68	0.23
	20.52 - 53.08	34.60 - 48.60	10.01 - 100.00	966.61 - 1029.09	0.00 - 192.75	0.00 - 33.98	0.00 - 95.11	0.00 - 3.23	0.00 - 5.82	0.00 - 1.26
December	31.19	42.68	83.42	993.02	3.81	4.79	10.50	0.34	0.60	0.16
	18.75 - 43.48	32.16 - 46.51	48.09 - 99.60	966.48 - 1021.19	0.00 - 65.93	0.00 - 29.31	0.00 - 68.13	0.00 - 2.66	0.00 - 5.22	0.00 - 0.75



**Appendix 2: Table of averages and minimum/maximum values at the Duck Flats buoy, by month.**

Month	Air Temperature (°F)	Water Temperature (°F)	Relative Humidity (%)	Barometric Pressure (%)	Solar Radiation (W/m <sup>2</sup> )	Wind Speed (knots)	Wind Gust (knots)	Significant Wave Height (ft)	Maximum Wave Height (ft)	Current Speed (knots)
January	17.75 3.81 - 34.39	41.27 33.30 - 44.83	77.91 10.86 - 100.00	992.19 953.29 - 1018.67	9.65 0.00 - 200.66	9.00 0.00 - 30.30	16.55 0.00 - 80.90	0.50 0.00 - 2.69	0.90 0.00 - 4.99	0.14 0.00 - 0.70
February	24.51 10.29 - 39.47	39.77 32.50 - 42.13	76.93 12.38 - 100.00	994.93 964.57 - 1019.60	24.92 0.00 - 333.36	5.89 0.00 - 28.46	10.83 0.00 - 66.17	0.29 0.00 - 2.14	0.52 0.00 - 3.71	0.12 0.00 - 0.55
March	29.97 14.09 - 51.96	40.65 32.02 - 43.13	58.99 15.90 - 100.00	1005.70 976.47 - 1037.18	104.42 0.00 - 630.10	6.95 0.00 - 31.10	14.23 0.00 - 78.30	0.22 0.00 - 1.73	0.41 0.00 - 3.07	0.13 0.00 - 0.84
April	37.95 18.96 - 49.77	44.05 39.47 - 50.36	74.58 21.97 - 100.00	1004.07 979.17 - 1025.10	145.99 0.00 - 787.33	3.53 0.00 - 19.57	7.29 0.00 - 46.42	0.09 0.00 - 1.06	0.18 0.00 - 1.70	0.09 0.00 - 0.52
May	46.03 33.36 - 57.67	47.34 38.69 - 53.87	80.39 27.24 - 98.50	1002.77 989.29 - 1020.53	161.07 0.00 - 816.81	4.32 0.00 - 23.97	12.07 0.00 - 54.04	0.37 0.03 - 1.34	0.68 0.06 - 2.18	0.25 0.03 - 0.51
June	50.91 41.79 - 62.56	48.28 40.88 - 54.64	84.53 59.24 - 98.10	1002.26 994.11 - 1011.15	186.44 0.00 - 839.45	4.81 0.00 - 23.83	12.72 0.00 - 54.35	-	-	0.14 0.00 - 0.77
July	53.96 44.37 - 78.12	49.47 37.97 - 59.95	87.15 23.19 - 100.00	1003.09 991.91 - 1014.06	160.91 0.00 - 875.80	3.53 0.00 - 22.12	8.82 0.00 - 55.24	-	-	0.14 0.00 - 0.72
August	52.49 43.35 - 75.22	49.22 38.99 - 56.84	89.20 27.67 - 100.00	997.72 978.77 - 1006.33	110.50 0.00 - 731.37	2.92 0.00 - 25.42	6.12 0.00 - 53.90	-	-	0.13 0.00 - 0.82
September	46.53 35.06 - 61.00	48.18 36.72 - 55.45	88.43 10.09 - 100.00	999.47 967.75 - 1021.05	69.23 0.00 - 553.97	2.58 0.00 - 19.90	4.26 0.00 - 54.04	0.06 0.00 - 0.51	0.11 0.00 - 1.15	0.13 0.00 - 0.71
October	39.97 25.21 - 55.20	46.76 39.26 - 52.92	80.48 10.84 - 100.00	1005.41 971.36 - 1036.23	37.05 0.00 - 500.47	3.87 0.00 - 25.31	6.66 0.00 - 61.40	0.11 0.00 - 1.47	0.20 0.00 - 2.56	0.12 0.00 - 0.95
November	32.40 14.68 - 49.33	42.74 37.27 - 47.50	79.14 13.65 - 100.00	1000.36 963.49 - 1030.19	12.49 0.00 - 260.51	5.09 0.00 - 30.98	7.12 0.00 - 65.72	0.07 0.00 - 0.86	0.14 0.00 - 1.73	0.12 0.00 - 0.77
December	28.86 13.50 - 40.86	41.91 32.10 - 46.36	86.27 10.22 - 100.00	992.52 961.57 - 1022.70	4.56 0.00 - 176.74	4.02 0.00 - 23.33	7.62 0.00 - 65.91	0.13 0.00 - 1.66	0.25 0.00 - 3.10	0.11 0.00 - 0.51